NUCLEAR STOPPING

IN HEAVY-ION COLLISIONS

Thesis submitted in partial fulfillment of the requirement for

The award of the degree of

MASTERS OF SCIENCE

IN

PHYSICS

Under the guidance of

Dr. Suneel Kumar

Submitted by

Maninder Kaur

Roll no. – 30704008

School of Physics and Material Science

Thapar University

Patiala – 147004 (PUNJAB),INDIA

CONTENTS

CERTIFICATE

This is to certify that Ms. Maninder Kaur, Roll No. 30704008 has worked on this thesis report as a partial fulfillment for award of the degree of MASTERS OF SCIENCE in physics. I certify that the matter embodied in this report is of candidate's own record and not submitted to any other university in any part or full form for the award of such a degree.

S Kumar 11/7/09

(Dr. Suneel Kumar)
Supervisor
SPMS, Thapar University
Patiala

Countersigned by:

O. Pandey

Dr. O.P.Pandey
(Prof. & Head)
School of Physics and Materials Science
Thapar University, Patiala.

R.K. Sharma 3/7/09

Dr. R.K. Sharma
Dean of academic Affairs
Thapar University
Patiala.

i

ACKNOWLEDGEMENT

Knowledge in itself is a continuous process. I would have never succeeded in completing my task without cooperation, encouragement and help provided to me by various personalities.

With deep sense of gratitude I express my sincere thanks to my worthy superviser, **Dr. Suneel Kumar**, for his valuable guidance in caring out work under his effective supervision, encouragement and cooperation.

I would like to give my thanks to **Dr. O. P. Pandey**, Professor and Head, School of Physics and Material Science, for his full motivation and appreciation to my work

I wish to express my thanks to **Mrs. Varinderjit Kaur** and **Mr. Sanjeev Kumar**, Research Scholars for the help and valuable suggestions whenever I needed out of their bust schedule.

All my friends at the School of Physics and Material Sciences are acknowledged for providing me a friendly atmosphere and encouraging me throughout this work. Their assistance and partnership were of great pleasure. Their views were very insightful and helpful.

I am deeply thankful to my family, their moral support and patience has bared fruit through completion of this Thesis which will result in award of the prestigious degree of M.Sc.

Above all I render my gratitude to the Almighty who bestowed self – confidence, ability, strength and path to me in accomplishing this work.

Date: *Maninder Kaur*

Place: Patiala *Roll No.* 30704008

ABSTRACT

A semi-classical transport model, namely, Isospin quantum molecular dynamics (IQMD) model, is employed to investigate the emission of free, light charged particles and degree of equilibrium or stopping reached in heavy ion collisions. We study the dependence of nuclear stopping Q_{zz} and R in intermediate energy heavy ion collisions on transverse momentum, rapidity, energy, N/Z and scaled impact parameter. For this study, simulations were carried out for the systems $^{52}Cr_{24}$ + $^{54}Ni_{28}$, $^{52}Cr_{24}$ + $^{56}Ni_{28,}$ $^{52}Cr_{24}$ + $^{58}Ni_{28,}$ $^{52}Cr_{24}$ + $^{60}Ni_{28,}$ $^{52}Cr_{24}$ + $^{62}Ni_{28}$ at different beam energies from 50 to 200 MeV/nucleon at reduced impact parameters i.e. at $\hat{b}$ = 0, 0.1, 0.2, 0.3 using soft equation of state (EOS) employed at symmetry energy E = 32 MeV/n. We find that the effect of N/Z on stopping is weak. It is shown that R and Q_{zz} behave as a global stopping parameter. Moreover, maximum stopping is obtained for low beam energies in the presence of symmetry energy in central collisions.

List of Figures:

List of table:

Chapter 1

Introduction

The nuclear physics (at low/intermediate/high energies) is one of the most extensively studied fields. With all the theoretical and experimental work, we are able to differentiate the nuclear physics into four different branches. One of the branch deals with the study of deconfinement and quark-gluon plasma. Second branch led to the study of low energy γ-ray spectroscopy. The third branch deals with the study of nuclear collectivity through giant resonances and lastly, the branch exploring the field of intermediate energy heavy-ion reaction. [1]

The traditional picture of the nucleus in low energy nuclear physics is that of interacting many-body systems of structure less, point like protons and neutrons. By low energy nuclear physics we understand the region of excitation energies δE smaller than the Fermi energy (ε_F =30-40 MeV) and momentum transfers δq ≤1/R, where R is the nuclear radius. The low energy heavy-ion reactions give unique possibility to look for the nuclear interaction, fusion-fission, cluster-radioactivity, formation of super heavy nuclei, the possibilities of synthesis of super heavy elements through the neutron rich radioactive beams, the halo nuclei etc. In other words, the low energy nuclear physics focus mainly on the structure of nuclei [2, 3].

. The situation changes as δE or δq is increased by several hundreds of MeV/nucleon upto a few GeV/nucleon, the domain of intermediate energy physics [3]. With the passage of time, one was able to accelerate the heavy-ion with bombarding energies comparable to its rest mass. This opened up new dimensions which are termed as intermediate and relativistic energy heavy-ion physics. At this point, explicit

mesonic degrees of freedom become directly visible. As mesons become important, nucleons begin to reveal their intrinsic structure.

Unified many-body treatments of the nucleus at low and intermediate energies are commonly based on the assumptions of nucleons and quasiparticles, interacting by the exchange of mesons. There are many phenomena which can be studied at intermediate energies i.e. multifragmentation, directed flow, elliptical flow, stopping parameters like: Quadrupole moment, stopping ratio R, sub threshold production of particles etc.

One of the main interests of the study of heavy-ion collisions is the investigation of the properties of nuclear matter at extreme densities and excitation energies [4-11]. These investigations include the production of secondary particles, the properties of particles in a (dense) nuclear medium, the compression and repulsion of dense nuclear matter, its equilibration during the reaction and its decay into fragments and single particles. On a macroscopic level the total energy of a dense nuclear system and its decomposition into thermal and compressional parts is related to the concept of the nuclear equation of state. Since a consistent derivation of the nuclear equation of state, e.g. the energy per nucleon as a function of density and temperature, is only possible in the low density limit, a reliable theoretical description is not at hand. On the other hand this quantity is of interest for many astrophysical questions and therefore its knowledge is highly desirable. Heavy ion reactions in combination with corresponding simulations using a variety of parametrizations of the equation of state are presently the only possible approach to study this process.

At temperatures of ~20-30 MeV/nucleon, we expect nuclear matter to undergo a second–order phase transition at the critical point. This is essentially due to the fact that the nuclear equation of state has a short-range repulsive and a long-range attractive component similar to a Vander Waals equation of state. We hope to achieve

these kinds of excitation energies by bombarding of heavy ions with multi-GeV protons, where the spectator matter is heated up, and by colliding heavy ions at beam energies around 100 MeV/nucleon, where the participants can in principle reach the necessary excitation energy.

Energy per nucleon E in cold nuclear matter can be represented as a sum of the energy of symmetric nuclear matter E_0 and a correction E_1 associated with the neutron-proton (np) imbalance:

$$E(\rho_n, \rho_p) = E_0(\rho) + E_1(\rho_n, \rho_p) . \qquad (1)$$

At small relative np asymmetries, on account of the np symmetry of nuclear interactions, the energy E must be quadratic in the asymmetry,

$$E_1 = E - E_0 \approx S(\rho)\left(\frac{\rho_n - \rho_p}{\rho}\right)^2 . \qquad (2)$$

Traditionally, both the energy E_1 and the coefficient of proportionality S in (2) are called the symmetry energy [12]. With (2), the energy in neutron matter, characterized by $\rho_n >> \rho_p$, is given by $E \approx E_0+S$. Pressure in cold nuclear matter is related to the energy per nucleon with $P = \rho^2 \partial E / \partial\rho$. For densities close to normal, $\rho \sim \rho_0$, because of the minimum in E_0, the pressure in neutron matter becomes dominated by the symmetry energy, $P \approx \rho^2 \partial S / \partial\rho$.

A prerequisite for the understanding of the high density and temperature phase of nuclear matter that might have prevailed in the initial stage of the reaction is the knowledge and the description of the final state that reflects the properties when the constituents cease to interact (freeze-out). The freeze-out conditions visible in the distributions of hadrons are very important since they allow testing concepts like equilibrium and stopping, and therefore are very useful as a constraint for all more elaborated theories. In the past, these studies were focused on the multifragmentation, that constitute free particles, fragments of different sizes as well as secondary particles

like pions or kions etc. Additional promising observable was anisotropy in the momentum distribution which include the directed in-plane flow (bounce off) or out of plane flow (squeeze out) of nucleons [11, 13]. One is also interested to understand the mechanism behind in-plane (attractive mean field) to out-of-plane (repulsive N-N scattering) emission at intermediate energies. This mechanism leads the matter from a fused state to total disassembly. Global stopping is found to explore this mechanism. It is an important quantity in determining the outcome of a reaction and may drastically vary with incident energy, mass of colliding nuclei and colliding geometry. This has been linked with the thermalization (equilibrium) in heavy ion collisions.

1.1 Nuclear stopping

There is considerable interest in the stopping power of nuclei at relativistic energies. The nuclear stopping power can be viewed as a measure of the degree to which the energy of the relative motion of the two colliding nuclei is transformed into other degrees of freedom [14]. The amount of nuclear stopping determines parameters, such as the energy and volume of the interaction region (and therefore energy density), which govern the reaction dynamics and the extent to which conditions might be favorable for formation of a high density, deconfined phase of matter. With increased nuclear stopping, increased thermalization of the incident energy, higher energy densities during the collisions and a combination of increased particle production and collective flow are expected. Therefore, an understanding of nuclear stopping measurements at the presently available collision energies should provide insight into the energy and baryon densities that will be reached in the future in nuclear collisions at higher energies experimented by FOPI group [15] at GSI (Germany) and INDRA group [16] at GANIL (USA).

It is important to investigate whether an equilibrium is reached or not for a colliding system in order to obtain correctly the information of equation of state (EOS) and the reaction mechanism. This problem has been studied extensively both

theoretically and experimentally [17-22]. Following the establishment of radioactive beam facilities in many laboratories, it has become possible to study neutron-rich (or proton-rich) nuclear collisions at intermediate energies. Therefore it is necessary to study the effect of isospin asymmetry on the equilibrium process in a colliding system. The sensitivity of nuclear stopping to the isospin dependence of the cross section was studied but the isospin dependence of the medium correction of two-body cross sections and the isospin asymmetry of the initial system were not tested [23]. As expected, the degree of equilibrium is influenced by the mean field, the medium correction of two-body cross section as well as the size of the colliding system.

The study of the isospin effect at intermediate energy heavy ion collisions can be used to get the information for the in-medium nucleon-nucleon (*NN*) cross section and isospin dependent mean field. It was found that the in-medium cross sections decreased with the density and increased slightly when the density was higher than normal nuclear density and the energy was higher than about 125A MeV (in the laboratory system). Concerning the nucleon-nucleon cross section, it is already known that up to hundreds MeV the free proton-neutron cross section is about 2–3 times larger than that of proton-proton (neutron-neutron's) [24] .The influence of the mean field is considered by taking the EOS to be the "soft" EOS ($\mathcal{K}$ = 200 MeV) and the "hard" EOS ($\mathcal{K}$ = 380 MeV) as well as with and without the isospin symmetry potential. The momentum dependence of the nuclear interaction in infinite cold nuclear matter does not influence on EoS, but they claim that the momentum dependent interaction (MDI) leads to an additional repulsion between nucleons in heavy-ion collisions [25,26]. Such MDI reduces the yield of pions and kaons substantially, while the transverse momentum transfer for beam energies 400A MeV increases. Therefore, the MDI leads the non-equilibrium effects in heavy-ion collisions and the determination of the EoS cannot be simply extracted from experimental data.

In nucleus-nucleus collisions, stopping can be seen as a shift of the rapidity distribution of the incident nucleons towards mid-rapidity, i.e. the centre-of-mass of the

collision. Thus, the shape of rapidity distributions provides key information in terms of the nuclear stopping power. Bauer *et al.* pointed out that in intermediate energy HIC, nuclear stopping power is determined by both the mean field and the in-medium nucleon-nucleon (*N*-*N*) cross section [27], but the mean field he used did not include symmetry potential. Recently Bass, Yennello, Johnston, Li, and co-workers suggested that the degree of approaching isospin equilibration provides a means to probe the mechanism and the power of nuclear stopping in HIC [28]. But it is not clear how the stopping power depends on the symmetry potential in the same collisions. There is a possibility to extract information on the in-medium *N*-*N* cross section in intermediate energy HIC by using nuclear stopping as a probe.

1.2 Review of the Experiments performed

We shall first summarize the experiments which are performed during last years and then, a brief discussion of various theoretical methods used around the world to pin down the Heavy-Ion collisions (HIC).

Experiments performed at LBL in the early 80's yield first 4π information of the final momentum distributions in heavy-ion reactions. The first experiments at Berkley served mainly to get the experimentalists and theoreticians aware of the problems from medium energy heavy-ion collisions to equation of state. Later on, several accelerators were built at Michigan State University (USA), GANIL (France), and at GSI (Germany) [1]. These experiments enable precise measurements on the emission of primary and secondary particles and therefore provide a stimulating challenge to the theoretical description of heavy ion collisions. The SIS (Heavy-ion synchrotron) accelerator at GSI is specially designed to study the heavy-ion collisions at intermediate energies. The MSU group at Michigan State University is very active in studying the fragment's spectra at lower side of the bombarding energies. The similar efforts are also made by the INDRA group at GANIL [29]. The ALADIN group at GSI has gone ahead and provided complete spectra of the fragments [30].

The FOPI and ALADIN group at GSI are studying the variety of reactions giving nearly all kinds of possibilities. It ranges from ^{12}C to ^{208}Pb and with incident energy between 100A and 1000A MeV [31-36]. A lot of physical conclusions are also drawn from these studies. If one goes through above experiments, one will notice that two different varieties (i.e. symmetric and asymmetric reactions merge). The symmetric reaction will generate high compression whereas asymmetric reaction will lead to heat or thermal energies. The aim of heavy target against light projectile is to look for the target multi-fragmentation whereas a heavy projectile on light target gives projectile fragmentation. Naturally, the physics at peripheral collisions is dominated by the spectator physics whereas the central collisions have a fireball dynamics.

Different experiments gave indications that the impact parameter can be closely related with the emission of charged particles, thus make it possible to extract the impact parameter experimentally. A large multiplicity of the charged particles is associated with central collisions which decrease with increase in impact parameter [37, 38, 39, 40]. If one deals with the intermediate mass fragment production at higher energies, one sees a rise or fall in the multiplicity of the fragments with a change in the impact parameter. Apart from these observations, the associated properties of fragments like collective flow, energy spectra, rapidity distributions are also investigated.

The nucleons are found to be emitted from participant zone whereas the heavy fragments are the remnants of spectators. The collective flow is found to increase with increase in the size of fragments. At very low incident energies, one finds negative sideward flow whereas at high incident energies, the flow is repulsive. This means that while going from low to high energies, the flow will disappear at some incident energy. This energy is termed as balance energy. It was also reported that this balance energy varies as $A^{-1/3}$ [41].

1.3 Review of theoretical models for Heavy-Ion collision

On the theoretical side, heavy ion collisions can be investigated with nuclear fluid dynamics and microscopically transport models. One of the most successful microscopic transport models is the Quantum Molecular Dynamics (QMD) model and its extension to relativistic energies, the Relativistic Quantum Molecular Dynamics (RQMD) model. (R)QMD simulations have predicted a wide variety of phenomena which later have been confirmed by experiment. Among these are the *collective flow* of nucleons, light and heavy fragments and of pions, the production of kaons as well as the *squeeze-out* of nucleons and pions perpendicular to the reaction plane. The improvement of the QMD/RQMD model and its application to future experiments at GSI, at the AGS and at CERN is of great importance for the further understanding of processes occurring in high energy heavy ion collisions.

A lot of comparisons have been made between experimental data and microscopic and macroscopic transport-theoretical calculations. Besides these microscopic models like SMM, VUU, BUU, AMD or FMD, the Quantum Molecular Dynamics approach (QMD) is a frequently used model. Theoretically, several models have been developed which makes the situation more complicated. The key point to remember is that heavy ion collisions involve very complicated non-equilibrium physics; therefore, its numerical modelling is not straight forward. Due to lack of free phase-space at low incident energies about 98% of the attempted collisions are blocked. The whole dynamics at low energies is governed by the mean field or by the mutual two and three body interactions. In contrary, the availability of large free phase-space at relativistic energy (>2A GeV) makes the Pauli principle's role quite small (roughly 4% collisions are blocked) and hence the dynamics of a reaction is governed by the cascade picture. On the other hand, both cascade and mean field picture emerges at intermediate energies.

The conventional theories like the time independent Hartree-Fock (TDHF) [42, 43, 44, 45] or its semi-classical version the so called Vlasov Equation (in phase space) are suitable at low energies where nucleon-nucleon collisions are negligible. Some attempts were made to extend the TDHF to take care of the residual nucleon-nucleon interactions which are responsible for the two body collisions (this was dubbed as ETDHF) and thus a new realization (named as Boltzmann-Uehling Uhlenbeck equation (BUU)) is used till date to study the large deviating problems of low, intermediate and relativistic heavy-ion collisions. The solution of BUU [46, 47] equation provides the time evolution of one-body distribution function in six dimensional phase-spaces. Due to one body nature, BUU cannot describe directly, for example, the multi-fragmentation phenomenon which involves the correlations between nucleons.

Naturally, one would like to have the methods where correlations and fluctuations among the nucleons can be preserved. The classical molecular dynamics (MD) [48, 49] approach (or the equation of motion), in principle, is capable of treating both the compression and the fragment formation. The molecular dynamics predicts the collective flow. It incorporates the complete classical N-body dynamics which is necessary to describe the formation of the fragments. Naturally, the simple classical molecular dynamics needs major refinements which should also include the quantum features. The quantum features play very important role at low energies. This approach was later extended which explicitly incorporates the N-body correlations, a nuclear equation of state and important quantum features like Pauli principle, stochastic scattering and particle production and was named as Quantum Molecular Dynamics (QMD) model [52-54]. The crucial quantum features like antisymmetrization etc. were implemented in approaches like Fermionic Molecular Dynamics (FMD) [50] and Antisymmetric Molecular Dynamics (AMD) [51]. The serious numerical problems have restricted the use of FMD and AMD approaches to light nuclei only. Several refinements and improvements were made over the original QMD [52-54]. These new versions were named as IQMD (isospin-QMD). IQMD [55-56] has been used for the analysis of collective flow effects of nucleons and pions taking isospin into consideration.

The rapidity distribution of the neutron-proton difference is a sensitive probe to the degree of equilibration with respect to the isospin degree of freedom. The rapidity spectra of particles can be reproduced by IQMD with a free nucleon-nucleon cross section for the most central collisions. The ratio of baryon rapidity distributions in isospin asymmetric collision systems shows incomplete mixing and partial transparency of the projectile and target nuclei at different beam energy. By using the isospin dependent quantum molecular dynamics model (IQMD), experiments have been performed to study the dependence of nuclear stopping Q_{ZZ}/A and R in intermediate energy heavy ion collisions on system size, initial N/Z, isospin symmetry potential and the medium correction of two-body cross sections.

From above discussion, it is clear that several theoretical tools are available. As our present interest is to understand the formation of fragments taking isospin into consideration, we shall study the dynamics of fragmentation using IQMD model. The IQMD model can produce the measured proton and deuteron rapidity spectra for the most central events, with very similar results for the option of a hard and soft equation of state. Nuclear stopping in heavy ion collisions (HIC) has been studied by means of rapidity distribution and asymmetry of nucleon momentum distribution in intermediate energy HIC, nuclear stopping power is determined by both the mean field and the in-medium nucleon-nucleon (*N*-*N*) cross section. The effects of both in-medium *N*-*N* cross section and symmetry potential on nuclear stopping shall be studied comparatively for colliding systems with different neutron-proton ratios in the beam energy ranging from 50 to 200 MeV/*u* by using an isospin dependent quantum molecular dynamics (IQMD) model. The nuclear stopping R and Q_{zz} can be used as a probe to extract information on the isospin dependence of the in-medium *N*-*N* cross section in HIC.

The dynamical models can follow the phase-space of nucleons and are capable of studying the various experimental observables. Note that all these dynamical models follow the time evolution of the nucleons only, and therefore, one needs a procedure to define the clusters. In a very simple picture, the nucleons were connected to a cluster using space correlation method. This method identifies two nucleons in the

same fragment if their centroids are less than some distance [57]. This method is also called as *Minimum Spanning Tree (MST)* method [57]. Recently, this method when coupled with QMD model failed to explain the observed fragment distribution obtained by ALADDIN group. This failure even led to the idea that the energy transferred in QMD from particle to spectator matter was not enough to break the spectator into pieces.

1.4 Objective and motive of the work:

Our objective is to study *Nuclear Stopping in Heavy- ion Collision at Intermediate energies.* In the present analysis, simulations were carried out using IQMD model for the systems $^{52}Cr_{24}$ + $^{54}Ni_{28}$, $^{52}Cr_{24}$ + $^{56}Ni_{28,}$ $^{52}Cr_{24}$ + $^{58}Ni_{28,}$ $^{52}Cr_{24}$ + $^{60}Ni_{28,}$ $^{52}Cr_{24}$ + $^{62}Ni_{28}$ at different beam energies from 50 to 200 MeV/nucleon at reduced impact parameters i.e. at $\hat{b}$ = 0, 0.1, 0.2, 0.3 using soft equation of state (EOS) employed at symmetry energy E = 32 MeV/n to study stopping for central and non central collisions. This can be used as a parameter to study nuclear thermalization. Here, we don't have any experimental data to compare our results. We will explore the Isospin effect on nuclear stopping by taking neutron deficient and neutron rich nuclei. We shall attempt to correlate the emission of light charged particles and degree of equilibrium reached in the reactions in the presence of symmetry energy. From the review, it is clear that, a complete knowledge of degree of stopping is very important. This arises during the compression stage, where in addition to compression, colliding nuclei heat the nuclear matter [58]. Moreover, the destruction of initial correlations, make the matter homogeneous and hence one have global stopping. More the initial correlations of nucleons are erased, better is the stopping and hence equilibrium is approached.

References

[1] Dr. Suneel Kumar , Ph.D. Thesis, P.U. Chandigarh (2000)

[2] W. Weise, A. M. Green, *Quarks and nuclei* (World Scientific, Singapore, 1985)

[3] C.Y. Wong, *Introduction to High-Energy Heavy-Ion Collisions* (World Scientific, Singapore, 1994).

[4] W. Scheid, R. Ligensa, and W. Greiner. Phys. Rev. Lett. **21**, 1479 (1968)

[5] L. P. Csernai and J. I. Kapusta. Phys. Reports **131**, 225 (1986)

[6] R. Stock. Phys. Reports **135**, 261 (1986)

[7] H. Stöcker and W. Greiner. Phys. Reports **137**, 277 (1986)

[8] R. B. Clare and D. Strottman. Phys. Reports **141**, 179 (1986)

[9] B. Schurmann, W. Zwermann and R. Malfiet. Phys. Reports **147**, 3 (1986)

[10] W. Cassing, V. Metag, U. Mosel and K. Niita. Phys. Reports **188**, 361 (1990)

[11] J. Aichelin. Phys. Reports **202**, 233 (1991)

[12] I. Bombaci and U. Lombardo, Phys. Rev. C **44**, 1892(1991)

[13] A. D. Sood and R. K. puri, Phys. Rev. C **69**, 054612 (2004); S. Kumar, M. K. Sharma, R. K. Puri, K. P. Singh and I. M. Govil, *ibid.,* **58**, 3494 (1998)

[14] Wolfgang Bauer, Gary D. Westfall, *Advances in Nuclear Dynamics 2 (Springer Publication,* 1996)

[15] J. P. Alard *et al.,* Phys. Rev. Lett. **69**, 889 (1992)

[16] J. Lukasik, et al. (INDRA collaboration), Phys. Rev. C **55**, 1906 (1997)

[17] J. Cugnon , T. Mizutani and J. Vandermeulen, Nucl. Phys. A **359**, 345 (1981)

[18] J. Randrup, Nucl. Phys. A **314**, 429 (1997)

[19] M Cubero, M Schonhofen, B. L. Frimen and W. Norenberg, Nucl. Phys. A **340**, 385

(1991)

[20] A. Lang, B. Blattel, V. Koch, Weber K, W. Cassing and U. Z. Mosel, Phys. A **340,** 287 (1991)

[21] Z. X. Li, Y. Z. Zhuo, Y. Q. Gu, *et al.,* Nucl. Phys. A **559**, 603 (1993)

[22] Z. X. Li, Y. Z. Zhuo, X. Z. Wu and M. Sano, J. Phys. G: Nucl. Part. Phys. **20,** 1829 (1994)

[23] J. Y. Liu, W. J. Guo, S. J. Wang, *et al*.,Phys. Rev. Lett. **86**, 975 (2001)

[24] K. Chen, Phys. Rev. 166, 949 (1968)

[25] B. A. Li and Udo W. Scroder, *Isospin Physics In Heavy-Ion Collisions at Intermediate Energies* (New York : Nova Science, 2001)

[26] I. Bombaci and U. Lombardo, Phys. Rev. C **44**, 892 (1991)

[27] W. Bauer, Phys. Rev. Lett. **61**, 2534 (1988).

[28] Jian-Ye Liu, Wen-Jun Guo, Phys Rev. Lett. **86,** 975 (2001)

[29] N. Marie *et al.,* Phys. Rev. C **58**, 256 (1998); W. Loveland *et al.,* Phys. Rev. C **59**, 1472 (1999); J. D. Frankland *et al.,* Nucl. Phys. A **689**, 940 (2001); S. Hundan *et al.,* Phys. Rev. C **67**, 064613 (2003); J. D. Frankland *et al.,* Phys. Rev. C **71**, 034607 (2005)

[30] C. A. Ogilvie *et al.,* Phys. Rev. Lett. **67**, 1214 (1991); J. Hubele, *et al.,* Phys. Rev. C **46**, R1577 (1992); M. Begemann-Blaich, *et al.,* Phys. Rev. C **48**, 610 (1993); G. F. Peaslee, *et al.,* Phys. Rev. C **49**, R2271 (1994); A. S. Botvina, *et al.,* Nucl. Phys. A **584**, 737 (1995); A. Schuttauf, *et al.,* Nucl. Phys. A **607**, 457 (1996); N. T. B. Stone *et al.,* Phys. Rev. Lett. **78**, 2084 (1997); A. S. Botvina *et al.,* Phys. Rev. C **74**, 044609 (2006)

[31] J. P. Alard et al., Phys. Rev. Lett. **69**, 889

[32] M. Begemann-Blaich et al., Phys. Rev. C **48**, 610

[33] G. Poggi et al., Nucl. Phys. A **586**, 755

[34] A. Schuttauf et al., Nucl. Phys. A **607**, 457

[35] J. P. hubbele et al., Z. Phys A **340**,263

[36] A. S. Botvina et al., Nucl. Phys. A **584**,737

[37] C. A. Ogilive et al., Phys. Rev. Lett **67**, 1214

[38] M. B. Tsang et al., Phys. Rev. Lett. **71**, 1502 (1993)

[39] R. T. de Souza et al., Phys. Rev. Lett. B **268**, 6 (1991)

[40] T. Li et al., Phys. Rev. Lett. **70**, 1924 (1993)

[41] J. J. Molitoris and H. stocker, Phys. Lett. B **162**, 47 (1985); G. F. Bertsch, W. G. Lynch and M. B. Tsang, Phys. Lett. B **189**, 384 (1987); D. Krofcheck *et al.,* Phys. Rev. Lett. **63**, 2028 (1989); J. Peter, Nucl. Phys. A **545**, 173 (1992); V. de la Mota *et al.,* Phys. Rev. C **46**, 677 (1992)

[42] H. Stöcker and W. Greiner, Phys. Rep. **137**, 277

[43] K. T. R. Davis and S. E. Koonin, Phys. Rev. C **23**, 2042

[44] A. K. Kerman and S. E. Koonin, Ann. Of Phys. **100**, 332

[45] P. Bonche, S. Koonin and J. W. Negele, Phys. Rev. C **13**, 1226

[46] G.F. Bertsch, H. Kruse and S. Das Gupta. Phys. Rev. C **29**, R673 (1984)

[47] J. Aichelin and G. Bertsch. Phys. Rev. C **31**, 1730 (1985)

[48] A. R. Bodmer, C. N. panos and A. D. Mackeller, Phys. Rev **22**, 1025

[49] R.J. Lenl, V. R. Pandharipande, G. Jacucci, Phys. Rev. C **31**, 1783

[50] H. Feldmeir, Nucl. Phys., A **515**, 147, A **586**, 493

[51] A. Ono , H. Hourichi, T. Maruyama, Phys. Rev. C **47**, 2652, Phys. Rev. C **51**, 299, Phys. Rev C **52**, 316

[52] J. Aichelin and H. Stöcker. Phys. Lett. B **176**, 14 (1986)

[53] G. Peilert, H. Stöcker, A. Rosenhauer, A. Bohnet, J. Aichelin and W. Greiner. Phys. Rev. C **39**, 1402 (1989)

[54] J. Aichelin, A. Rosenhauer, G. Peilert, H. Stocker, and W. Greiner. Phys. Rev. Lett. **58**, 1926 (1987)

[55] C. Hartnack. PhD thesis, GSI-Report 93-5 (1993)

[56] C. Hartnack, L. Zhuxia, L. Neise, G. Peilert, A. Rosenhauer, H. Sorge, J. Aichelin, H. Stocker, and W. Greiner. Nucl. Phys. A **495**, 303 (1989)

[57] J.singh, S. Kumar and R. K. Puri, Phys. Rev. C **62**, 044617 (2000); *ibid.,* Phys. Rev. C **65**, 024602 (2002)

[58] R. K. Puri, C. Hartnack and J. Aichelin, Phys. Rev. C **54**, R28 (1996); P. B. Gossiaux, R. K. Puri, C. Hartnack and J. Aichelin, Nucl. Phys. A **619**, 379 (1997)

Chapter 2

Methodology

2.1 Introduction

The study of intermediate energy heavy-ion collision needs correct treatment of the real and imaginary parts of nuclear interactions. The real part influences the trajectory of nucleons whereas the imaginary part deals with the nucleon-nucleon collisions. Presently the microscopic models can be subdivided into two classes: Those which follow the time evolution of the one-body phase space distribution and those which are based on *n*-body molecular dynamics or cascade schemes. We will first present Isospin dependent Boltzmann-Uehling-Uhlenbeck (IBUU) model, the Quantum Molecular dynamics (QMD) model and its extension i.e. Isospin Quantum Molecular Dynamic Model (IQMD). Then we will discuss method of clusterization.

2.2 Boltzmann- Uehling Uhlenbeck (BUU) Model

The microscopic transport models for the one-body Wigner phase space density distribution obtained different names although they solve the same equation. They differ in the technical realization, i.e. the computer program, and are known as Vlasov-Uehling-Uhlenbeck (VUU) model [1, 2] (or BUU [1, 3], LV [4]). They solve the following transport equation for the one-body Wigner density $f(\boldsymbol{r}; \boldsymbol{p}; t)$ in the limit $\hbar \longrightarrow 0$:

$$\frac{\partial f}{\partial t} + v.\nabla_r f - \nabla_r U.\nabla_p f = -\frac{1}{(2\pi)^6}\int d^3p_2\, d^3\dot{p}_2 d\Omega\, \frac{d\sigma}{d\Omega}\, v_{12} \times \{[f f_2 (1-\dot{f}_1)(1-\dot{f}_2) - \dot{f}_1\dot{f}_2 (1-f)(1-f_2)] \times (2\pi)^3 \delta^3 (p + p_2 - p_1' - p_2')\} \quad (2.1)$$

The left hand side of this equation is the total differential of f with respect to the time assuming a momentum independent potential U. This potential is calculated self consistently and corresponds to the real part of the Bruckner G-matrix, usually a

$$U = \alpha\left(\frac{\rho}{\rho_0}\right) + \beta\left(\frac{\rho}{\rho_0}\right)^{\gamma} \qquad (2.2)$$

Skyrme-parametrization of the real part of the G-matrix is employed, where ρ is the nuclear density which is frequently measured in units of the saturation density ρ_0 of cold nuclear matter.

The right hand side of (2.1) contains a Boltzmann collision integral, which is identified with the imaginary part of the G-matrix. This part describes the influence of binary hardcore collisions, where the term with $f f_2$ describes the loss of particles (in a phase space region) and the term with $\bar{f}_1\bar{f}_2$ the gain term due to collisions feeding the considered phase space region. The right hand side denotes the collision integral which also include the Pauli blocking. This equation is solved by test particle method. Here the phase-space of each nucleon is represented by large number of pseudo-particles (called test particles). In its numerical implementation, the above equation reduces to a set of 6 $\times$ (A_T + A_P) $\times$ N couple of first order differential equation in time. Here N is the number of test particles per nucleon and A_T and A_P are the target and projectile, respectively. The test particle method replaces the expectation value of a single particle observable:

$$\langle O(t)\rangle = \int f(r,p,t)\, O(r,p)\, d^3r d^3p \qquad (2.3)$$

by Monte-Carlo integration

$$\langle O(t)\rangle = \frac{1}{n(A_T + A_P)} \sum_{i=1}^{n(A_T + A_P)} O(r_i(t), p_i(t)) \qquad (2.4)$$

With $r_i(t)$ and $p_i(t)$ denote the points in phase space which are distributed according to f(r, p, t)

$$f(r,p,t) = \lim_{n\to\infty} \frac{1}{n(A_T + A_P)} \sum_{i=1}^{n(A_T+A_P)} \delta\big(r - r_i(t)\big)\,\delta(p - p_i(t)) \qquad (2.5)$$

It is obvious that a large number of test particles will be needed to avoid the numerical noise. These test particles are treated as classical point particles. In recent calculations, one has also succeeded to use the Gaussian wave packet [5] for test particles. These particles are then propagated under the classical Hamiltonian's equations of motion

$$\dot{p}_i = -\frac{\delta(H)}{\delta r_i} \qquad (2.6)$$

$$\dot{r}_i = \frac{\delta(H)}{\delta p_i} \qquad (2.7)$$

One should keep in mind that the forces acting on the test particles are calculated from the entire distribution including test particles from all events, hence the *n* parallel events are not independent and event-by-event correlations cannot be analyzed within this one-body transport models. In the limit $n \to \infty$ the distribution of these propagated test particles at the time *t* represents the one-body distribution function. Any one-body observable can be calculated by averaging the values weighted with the distribution function. In brief, the BUU model is able to explain the one-body observables like collective flow, stopping and particle spectra [5], but, fluctuations and correlations [6], such as the formation of fragments or the description of two-particle correlations in relativistic heavy ion collisions, are beyond the scope of a transport model based on a one-body distribution function.

2.3 Isospin-Dependent Boltzmann-Uehling-Uhlenbeck Model (IBUU)

In this model, the initial positions of protons and neutrons in the colliding nuclei are determined according to their density distributions predicted by the relativistic mean-field (RMF) theory. Their initial momenta are then taken to have a uniform distribution

inside the neutron or proton Fermi sphere with its Fermi momentum determined from the local density using the Thomas-Fermi approximation. The Isospin effects are included through the isospin-dependent total and differential nucleon-nucleon cross sections, the different Pauli blockings for protons and neutrons, the symmetry potential, and the Coulomb potential for protons. For nucleon-nucleon cross sections, we use as default the experimental values in free space, in which the neutron-proton cross section is about a factor of 3 larger than the neutron-neutron or proton-proton cross section. The IBUU transport model [7] treats explicitly protons and neutrons. It also includes an asymmetry term in the nuclear mean-field potential and different scattering cross sections for protons and neutrons. The nuclear mean-field potential is parameterized as

$$U(\rho,\tau_z) = U_0(\rho) + U_{asy}(\rho,\tau_z) \tag{2.8}$$

Where

$$U_0(\rho) = \alpha\left(\frac{\rho}{\rho_0}\right) + \beta\left(\frac{\rho}{\rho_0}\right)^{\sigma} \tag{2.9}$$

and

$$U_{asy}(\rho,\tau_z) = C\,\frac{\rho_p-\rho_n}{\rho_0}\,\tau_z \tag{2.10}$$

In the above, ρ_0 is the normal nuclear matter density; ρ, ρ_n and ρ_p are the nucleon, neutron, and proton densities, respectively and τ_z equals 1 for proton and -1 for neutron. For the strength of the asymmetry potential, we take C = 32 MeV. For nucleon-nucleon scatterings, both elastic and inelastic channels are included by using the experimentally measured cross sections with explicit isospin dependence. An approach which goes beyond a one-body description is the Quantum Molecular Dynamics (QMD) model [9-14].

2.4 Quantum Molecular Dynamics (QMD) Model

The QMD model [9-14] is an *n*-body theory which simulates heavy ion reactions at intermediate energies on an event by event basis. Taking into account all

fluctuations and correlations has basically two advantages: i) many-body processes, in particular the formation of complex fragments are explicitly treated and ii) the model allows for an event-by-event analysis of heavy ion reactions similar to the methods which are used for the analysis of exclusive high acceptance data.

Quantum Molecular Dynamics is introduced to avoid such problematic descriptions like the test-particle approach of the Vlasov-like models. The Vlasov term with the potential U in equation 2.1 describes a mean-field to which all particles contribute by their interaction with all the other particles. The averaging over parallel ensembles washes out the particle correlations. Therefore, these models do not include fluctuations.

The QMD model [9-14] contains the following ingredients: short-range interaction (hard-core repulsion), stochastic scattering with energy- and angle-dependent cross sections, inelastic collisions and particle production, and Fermi motion of the nucleons in the ground state as well as the consideration of the quantum effect of the Pauli principle. QMD is a microscopic description of heavy-ion collisions, similar to the Vlasov- like models of the preceding section (BUU model). In order to describe the isospin effects on the dynamical process of HIC, quantum molecular dynamics [11] should be modified properly: (1) the density-dependent mean field should contain the correct isospin-dependent terms including symmetry potential and Coulomb potential, (2) the in-medium *N*-*N* cross section should be different for neutron-neutron (proton-proton) and neutron-proton collisions, and finally, (3) Pauli blocking should be counted by distinguishing neutron and proton. In addition, the initial condition of the ground state of two colliding nuclei should also contain Isospin information.

2.5 Isospin Quantum Molecular Dynamics Model (IQMD)

The Molecular-Dynamics (MD) model attempts to describe the propagation of an N-body system with N-body correlations. This model is based on a purely classical

theory. For comparison with the experimental results of this thesis an extension of the microscopic QMD model is used. The IQMD [15,16] contains Isospin degrees of freedom and free pion propagation. IQMD has been used for the analysis of collective flow effects of nucleons [17, 18] and pions [19, 20]. The original IQMD program was developed further to include momentum dependent interactions.

Numerical structure: The IQMD model consists of three major parts, namely

i) The initialization of projectile and target,

ii) The propagation of nucleons, resonances and newly produced particles due to their mutual potential interactions, and

iii) The hard collisions according to the energy dependent cross section for the various channels together with the Pauli-blocking.

For the propagation the description of the potential(or to be more exact of the real part of the Brückner G-matrix) is of crucial importance. The solution of the transport equations for the *N*-body distribution function is done in the following way:

1. Projectile and target are initialized. For each of these nuclei the nucleons initialized according to a distribution $f(r; p; t = 0)$. This distribution is essentially constrained by the requirement to reproduce the ground state properties of the two nuclei, i.e. radii, binding energies.

2. The particles are propagated using Hamilton's equations of motion (2.6 & 2.7) with a given Hamiltonian $\langle H \rangle$.

3. Two particles close in coordinate space may perform a collision. The particles change their momenta respecting the Pauli principle.

The input into the program may be subdivided into three classes of parameters

Reaction parameters: projectile and target masses (and charges), bombarding energy, impact parameter. They define the whole kinematics of a single event.

Physics Parameters: interaction range, potential parameters, in medium cross sections and decay widths, etc. They correspond to a detailed description of interactions and may be changed within a reasonable range. Finally their deduction is a particular goal of the comparison between calculation and experiment.

Technical parameters: time step size, initial distance, cutoff parameters, maximum collision distance, etc. They are used to perform effective calculations on a computer. The observables should not depend on them.

If all these parameters are fixed the calculation of a single event can be performed in the following way:

- Initialize projectile and target nuclei in their “ground state" as mentioned above,
- Propagate the constituents of the system according to their mutual potential and hard scattering interactions, this includes
  - Calculation of interaction densities, forces and the Hamiltonian
  - Propagation of all particles according to Hamilton's equation of motion
  - Perform all collisions within this time step. Decide for each collision whether its final state is Pauli blocked. If this is the case: keep momenta of collision partners unchanged, otherwise change momenta according to the angular distribution of this particular channel.
- Output of information (coordinates, momenta, scattering partners, . . .) about the intermediate reaction stages and output of the final phase-space configuration (which would correspond to the freeze-out configuration in a thermal picture).

2.5.1 Formal derivation of the transport equation

In IQMD each nucleon is represented by a coherent state of the form (we set ħ, c = 1) which are characterized by 6 time-dependent parameters, r_i and p_i, respectively.

$$\phi_i(x_i; t) = \left(\frac{2}{L\pi}\right)^{3/4} e^{-(x_i - r_i(t))^2/L}\, e^{i x_i p_i(t)} \qquad (2.11)$$

The parameter L, which is related to the extension of the wave packet in phase space, is fixed. The total *n*-body wave function is assumed to be the direct product of coherent states (2.11)

$$\Phi = \prod_i \phi_i (x_i, r_i, p_i, t) \tag{2.12}$$

Note that we do not use a Slater determinant (with $(A_p + A_t)!$ summation terms) and thus neglect antisymmetrization. First successful attempts to simulate heavy ion reactions with antisymmetrized states have been performed for small systems [21, 22]. How to incorporate cross sections into a antisymmetrized molecular dynamics is not yet known. This limits its applicability to very low beam energies.

The initial values of the parameters are chosen in a way that the ensemble of $A_T + A_P$ nucleons gives a proper density distribution as well as a proper momentum distribution of the projectile and target nuclei.

The equations of motion of the many-body system are calculated by means of a generalized variational principle: we start out from the action [23]

$$S = \int_{t_1}^{t_2} L[\phi, \phi^*]\, dt \tag{2.13}$$

With the Lagrange functional L

$$L = \langle \phi \left| i\hbar \frac{d}{dt} - H \right| \phi \rangle \tag{2.14}$$

where the total time derivative includes the derivation with respect to the parameters. The Hamiltonian *H* contains a kinetic term and mutual interactions V_{ij} , which can be interpreted as the real part of the Bruckner G-matrix supplemented by the Coulomb interaction. We will later on describe the components of *H* in detail. The time evolution of the parameters is obtained by the requirement that the action is stationary

under the allowed variation of the wave function. This yields an Euler-Lagrange equation for each parameter.

If the true solution of the Schrodinger equation is contained in the restricted set of wave function $\phi_i(x_i; t)$ (with parameters $\boldsymbol{r}_i$; $\boldsymbol{p}_i$) this variation of the action gives the exact solution of the Schrodinger equation. If the parameter space is too restricted we obtain that wave function in the restricted parameter space which comes closest to the solution of the Schrodinger equation. Note that the set of wave functions which can be covered with special parameterizations is not necessarily a subspace of Hilbert-space, thus the superposition principle does not hold.

For the coherent states and a Hamiltonian of the form $H = \sum_i T_i + \frac{1}{2}\sum_{ij} V_{ij}$ (T_i = kinetic energy, V_{ij} =potential energy) the Lagrangian and the variation can easily be calculated and we obtain:

$$L = \sum_i \left[-\dot{r}_i p_i - T_i - \frac{1}{2}\sum_{j \neq i} \langle V_{ik} \rangle - \frac{3}{2Lm} \right] \tag{2.15}$$

Variation yields:

$$\dot{r}_i = \frac{p_i}{m} + \nabla_{pi} \sum_j \langle V_{ij} \rangle = \nabla_{pi} \langle H \rangle \tag{2.16}$$

$$\dot{p}_i = -\nabla_{ri} \sum_{j \neq i} \langle V_{ij} \rangle = -\nabla_{ri} \langle H \rangle \tag{2.17}$$

with $\langle V_{ij} \rangle = \int d^3 x_1 d^3 x_2 \phi_i^* \phi_j^* V(x_1, x_2) \phi_i \phi_j$. These are the time evolution equations which are solved numerically. Thus the variational principle reduces the time evolution of the *n*-body Schrodinger equation to the time evolution equations of 6. ($A_P + A_T$) parameters to which a physical meaning can be attributed. The equations of motion for the parameters r_i and p_i are given in equations 2.6 and 2.7. The numerical solution can be treated in a similar manner as it is done in classical molecular dynamics. Trial wave

functions other than the Gaussians in (2.15), yield more complex equations of motion for other parameters and hence the analogy to classical molecular dynamics is lost. If $\langle H \rangle$ has no explicit time dependence, QMD conserve energy and momentum by construction.

2.5.2 The relation to the nuclear equation of state

One strong motivation for the numerical simulation of nuclear stopping in heavy ion reactions is the possibility to investigate effects of the underlying nuclear equation of state on the dynamics. IQMD is a model for non-equilibrium dynamics with mutual interactions among the constituents and therefore does not contain any parameterization of the nuclear equation of state in terms of an explicit relation between number density, temperature and the energy density. In equilibrium and in the thermodynamic limit ($n \to 1$), however, such a functional relation can be deduced from the nucleon-nucleon potentials and the cross-sections employed in the model. For the description of the energy per nucleon as a function of density (assuming $T = 0$) usually Skyrme type parameterizations (see eq.2.1) are used. This generalized equation uses three parameters α, β, γ; two of them are fixed by the constraint that the total energy should have a minimum at the saturation density $\rho = \rho_0$ with a value of E/A = -16 MeV which corresponds to the volume energy in the Bethe-Weizsacker mass formula. Together with the condition that a free particle has no binding energy; there remains one degree of freedom. The third parameter is fixed by the nuclear compressibility, which is the second derivative of the energy at the minimum with respect to the density:

$$\kappa = 9\rho^2 \frac{\partial^2}{\partial \rho^2} \left(\frac{E}{A}\right) \qquad (2.18)$$

Two different equations of state are commonly used: A hard equation of state (H) with a compressibility of κ =380 MeV and a soft equation of state (S) with a compressibility of κ =200 MeV [1,2]. The parameters can therefore be chosen in such a way that a hard or soft eos is obtained for the infinite matter case. It should again be noted that the

parameters of the potentials allow a relation to the nuclear equation of state (eos) but that the microscopic description works as well for systems far off from equilibrium where no eos can be defined. The nuclear equation of state can only be defined as the bulk properties in the limit of an infinite system: The concept of the nuclear equation of state as discussed here does only make sense for large macroscopic systems in (at least local) equilibrium.

2.5.3 Potentials used in IQMD

A total Hamiltonian function with a kinetic energy T and a potential energy V is given by

$$H = T + V = \sum_i \frac{\vec{p_i}^2}{2m_i} + \sum_i \sum_{j>i} \int f_i(\vec{r}, \vec{p}, t) V^{ij} f_j(\vec{r}, \vec{p}, t)\, d\vec{r}\, d\vec{r}\, d\vec{p}\, d\vec{p} \qquad (2.19)$$

The potential in equation 2.19 is the sum of the following specific elementary potentials,

$$V = V_{loc} + V_{Yuk} + V_{Coul} + V_{mdi} + V_{sym} \qquad (2.20)$$

with the local hard-core repulsion,

$$V_{loc} = \sum_i \sum_{j>i} t_1\, \delta(\vec{r_i} - \vec{r_j}) + \sum_i \sum_{j>i} \sum_{k>j} t_2\, \delta(\vec{r_i} - \vec{r_j})\, \delta(\vec{r_i} - \vec{r_k}), \qquad (2.21)$$

The Yukawa long-range term,

$$V_{Yuk} = \sum_i \sum_{j>i} t_3 \frac{e^{\frac{|\vec{r_i} - \vec{r_j}|}{a}}}{\frac{|\vec{r_i} - \vec{r_j}|}{a}}, \qquad (2.22)$$

The Yukawa potential in IQMD V_{Yuk} is very short ranged and weak. Additional attractive Yukawa forces hence modify the EOS. Yukawa forces stabilize the nuclei because of the increase of the interaction range as compared to a δ-like Skyrme

potential. Thus nucleons notice earlier that they will arrive at the surface and are more effectively decelerated as without this potential. In addition the fluctuations are reduced. The Coulomb term with only a mean value for the nucleon charge because QMD does not know the Isospin of the particles,

$$V_{Coul} = \frac{Z}{A} \sum_i \sum_{j>i} \frac{e^2}{|\vec{r}_i - \vec{r}_j|} \tag{2.23}$$

and the momentum dependent interacion

$$V_{mdi} = \sum_i \sum_{j>i} t_4 \ln\left(1 + t_5 \left(\vec{p}_i - \vec{p}_j\right)^2\right) \delta\left(\vec{r}_i - \vec{r}_j\right) \tag{2.24}$$

The IQMD-model offers rather stable density distributions and good energy conservation, however for the price of nucleon evaporation and improper binding energies (E_{bind} ≈ 4-5 MeV/nucleon for heavy nuclei instead of 8 MeV/nucleon). In addition to the potential used in QMD (eq. 2.20), a symmetry potential between protons and neutrons corresponding to the Bethe-Weizsacker mass formula has been included

$$V_{sym}^{ij} = t_6 \frac{1}{\rho_0} T_{3i} T_{3j} \delta(r_i - r_j) \tag{2.25}$$

where T_{3i} and T_{3j} denote the isospin projections of particles *i* and *j*. Other baryonic potentials like V_{loc} and V_{mdi} are defined isospin-independent like in all other flavors.

The parameters are propagated under the total interaction calculated by the Hamiltonian equations of motion 2.6 and 2.7. Parameters used in equation 2.21 to 2.24 are in table 2.1.

(I)QMD parameters		
t_3	15	MeV
t_4	1.57	MeV
t_5	$5 \cdot 10^{-4}$	MeV^{-2}
t_6	25	MeV
a	1.5	fm

Table 2.1: IQMD parameters used in equation 2.21 to 2.24

The interaction potential is determined during initial calculations as follows:

$$V = V_{loc} + V_{Yuk} + V_{Coul} + V_{mdi} + V_{sym}^{ij} \qquad (2.26)$$

2.5.4 Initialisation in IQMD

In IQMD the centroids of the Gaussians in a nucleus are randomly distributed in a phase space sphere ($r \leq R$ and $p \leq p_F$) with $R = R_0.A^{1/3}$fm corresponding to a ground state density of $\rho_0 = 0.17$ fm^{-3}. The Fermi momentum p_F depends on the ground state density. For $\rho_0 = 0.17$ fm^{-3} it has a value of about $p_F \approx 268$ MeV/c. In IQMD the momenta are uniformly distributed within a momentum sphere $p \leq p_{Fermi} \sim 268$ MeV/c without further local constraints. Therefore it may happen that nucleons close to the surface, where the local potential energy is low, are unbound initially. It gives, however, a reduced binding energy per nucleon as compared to the Weizsäcker mass formula. Hence the initialized nuclei are less stable against spurious particle evaporation. Finally it should be noted that IQMD performs a Lorentz contraction of the nucleus coordinate distribution and which becomes important for higher energies i.e. for > 1 GeV/ nucleon .

2.5.5 Interaction range in IQMD:

The interaction range parameter L [24] influences the interaction density for finite systems. For (homogeneous) infinite nuclear matter the density (and thus the potential

energy) does not depend anymore on the extension of the Gaussian wave packets. Thus, the equation of state of infinite nuclear matter is independent of *L*. In finite matter *E*=*A* also depends on *L*. Thus even two parameterizations which yield the same EOS may produce different results for the reaction of two heavy ions. Therefore we have to adjust *L* to have reasonable surface properties. In order to allow a physical interpretation *L* should be in the order of the size one expects for the range of the nuclear interaction. There exists a range of values for *L* [24], which allows fixing these properties. Larger values of *L* increase the effective range of the interaction and thus lead to some smearing of fluctuations, which are stronger for more located wavepackets (small values of *L*). The Gaussian width can be regarded as a description of the interaction range of a particle. Its influence disappears for infinite nuclear matter whereas for finite systems it may play a non negligible role. In IQMD the Gaussian width can be used as an optional input parameter. The system dependence of *L* in IQMD has been introduced in order to obtain maximum stability of the nucleonic density profiles. As an example for Au + Au a value of $L = 8.66\ \mathrm{fm}^2$ is chosen, for Ca + Ca and lighter nuclei $L = 4.33\ \mathrm{fm}^2$.

2.5.6 Inclusion of collisions

Two particles collide if their minimum distances *d*, i.e. the minimum relative distance of the centroids of the Gaussians during their motion, in their CM frame fulfills the requirement:

$$d \leq d_0 = \sqrt{\frac{\sigma_{tot}(\sqrt{s})}{\pi}}, \qquad (2.27)$$

where the cross section is assumed to be the free cross section of the regarded collision type (*N* - *N*, *N* - *Δ*,. . .). Here $\sigma_{tot}(\sqrt{s})$ represents the total nucleon-nucleon cross-section and $\sqrt{s}$ is the center-of-mass energy. Here cross-section is divided into elastic and inelastic parts which depend on the center-of-mass energy available to the colliding pair of nucleons. For elastic channels, we use the total and differential cross-section as:

$$\sigma_{nn}^{(el)}(\sqrt{s}) = \begin{cases} 55\ (mb), & if\ \sqrt{s} < 1.8993; \\ \frac{35}{1+100(\sqrt{s}-1.8993)} + 20, & if\ \sqrt{s} \geq 1.8993; \end{cases} \quad (2.28)$$

With $\sqrt{s}$, the nucleon-nucleon center-of-mass energy given by

$$\sqrt{s} = \sqrt{(E_1 + E_2)^2 - (p_1 + p_2)^2} \quad (2.29)$$

Here E_i and p_i are, respectively, the energy and momentum of i^{th} nucleon.

For inelastic channels, the total cross-section is parameterized as:

$$\sigma_{nn\to n\Delta}^{(in)}(\sqrt{s}) = \begin{cases} 0, & if\ \sqrt{s} < 2.015 \\ \frac{20(\sqrt{s}-2.015)^2}{0.015+(\sqrt{s}-2.015)^2}, & if\ \sqrt{s} \geq 2.015 \end{cases} \quad (2.30)$$

If two particles scatter, the direction of the final momenta will be distributed randomly in such a way that the distribution of many identical collisions corresponds to the measured cross section. An earlier collision (e.g. at the point when the distance is sufficient to fulfill the distance condition) could cause stronger acausalities. It will also reduce the mean free path and thus enlarge stopping and flow [15]. The cross section is reduced to an effective cross section by the Pauli-blocking [26]. For each collision the phase space densities in the final states are checked in order to assure that the final distribution in phase space is in agreement with the Pauli principle ($f \leq 1$). If the collision is not allowed the particles remain at their original momenta. The final phases space fractions P_1 and P_2 which are already occupied by other nucleons are determined for each of the scattering baryons. The collision is then blocked with probability

$$P_{block} = 1 - (1 - P_1)(1 - P_2) \quad (2.31)$$

Pauli blockers of VUU and QMD show efficiencies of about 94-96 %, i.e. a single ground state nucleus with Fermi momentum would show a blocking rate of this amount.

Nevertheless the problem of Pauli blocking causes a limitation of the calculated system to have not less incident energy than about the Fermi energy.

2.6 Method of Clustrization

Minimum Spanning Tree (MST) method

The *MST* method is the most extensively method that is used to clusterize the nucleons [27]. In *MST* method, two nucleons share the same fragment if their centroids are closer than a distance d_{min},

$$|\vec{r}_i - \vec{r}_j| \leq d_{min} \tag{2.31}$$

where $\vec{r}_i$ and $\vec{r}_j$ are the spatial positions of both nucleons. The value of d_{min} can vary between 2-4 fm. It has small effect on multifragmentation [27]. However, this method cannot address the question of time scale as it will give a big fragment at the time of density when the interactions between the nucleons are still active. It is worth mentioning that this method can only be used to analyze asymptotic configurations in which the fragmenting system can be viewed as a very dilute mixture of free particles and almost equilibrated fragments.

References

[1] H. Kruse, B. V. Jacak, and H. Stöcker, Phys. Rev. Lett. **54**, 289 (1985)

[2] J. J Molitoris and H. Stocker, Phys. Rev C **32**, R346 (1985)

[3] G. F. Bertsch, H. Kruse and S. Das Gupta, Phys. Rev. C **29**, R673 (1984)

[4] C. Gregoire, B. Remaud, F. Sebille, L. Vinet, and Y. Raffray, Nucl. Phys. A **465**, 317 (1987)

[5] P. Ring and P. Schuk, *The nuclear many-body problem*, (Springer-Verlog, 1980); G. F. Bertsch and S. D. Gupta, Phys. Rep. **160**, 189 (1988); G. F. Bertsch, H. Kruse and S. D. Gupta, Phys. Rev. C **29**, 673 (1984); C. Gregoire, B. Remaud, F. Sebille, L. Vincet and Y. Raffay, Nucl. Phys. A **465**, 317 (1987); W. Bauer, Prog. Part. Nucl. Phys. **30**, 45 (1993); T. Reposeur, V. de la Mota, F. Sebille and C. O. Dorso, Z. Phys A **357**, 79 (1997)

[6] C. Gale, G. F. Bertsch and S. D. Gupta, Phys. Rev. C **35**, 1666 (1987); C. Gale, G. M. Welke, M. Prakash, S. J. Lee and S. D. Gupta, Phys. Rev. C **41**, 1545 (1990); Q. Pan and P. Danielewicz, Phys. Rev. Lett. **70**, 2062 (1993); J. Zhang, S. D. Gupta and C. Gale, Phys. Rev. C **50**, 1617, (1994);

[7] B. A. Li, C.M. Ko, and W. Bauer, Int. Jour. Phys. E **7**, 147 (1998).

[8] V. Greco, A. Guarnera, M. Colonna and M. D. Toro, Phys. Rev. C **59**, 810 (1999).

[9] C. Gregoire, B. Remaud, F. Sebille, L. Vinet, and Y. Raffray, Nucl. Phys. A **465**, 317 (1987)

[10] J. Aichelin and H. Stöcker, Phys. Lett. B **176**, 14 (1986)

[11] G. Peilert, H. Stöcker, A. Rosenhauer, A. Bohnet, J. Aichelin and W. Greiner. Phys. Rev. C **39**, 1402 (1989)

[12] J. Aichelin, A. Rosenhauer, G. Peilert, H. Stöcker, and W. Greiner. Phys. Rev. Lett. **58**, 1926 (1987)

[13] J. Aichelin. Phys. Reports **202**, 233 (1991)

[14] G. Peilert, A. Rosenhauer, J. Aichelin, H. Stöcker, and W. Greiner, Phys. Rev. C **39**, 1402 (1989).

[15] Ch. Hartnack. PhD thesis, GSI-Report 93-5 (1993)

[16] Ch. Hartnack, L. Zhuxia, L. Neise, G. Peilert, A. Rosenhauer, H. Sorge, J. Aichelin, H. Stöcker, and W. Greiner. Nucl. Phys. A **495**, 303 (1989)

[17] Ch. Hartnack, J. Aichelin, H. Stöcker and W. Greiner, Mod. Phys. Lett. A 9, 1151 (1994)

[18] Ch. Hartnack, J. Aichelin, H. Stöcker and W. Greiner, Phys. Lett. B **336,** 131 (1994)

[19] Ch. Hartnack, H. Stöcker and W. Greiner, In H. Feldmeier, editor, Proc. Of the *International Workshop On Gross Properties of Nuclei and Nuclear Excitation, XVI, Hirschegg, Kleinwalsertal, Austria (1998)*

[20] S. A. Bass, C. Hartnack, H. Stöcker and W. Greiner, phys. Rev. C **51,** 3343 (1994)

[21] H. Feldmeier. Nucl. Phys. A **515**, 147 (1990)

[22] A. Ono, H. Horiuchi, T. Maruyama and A. Ohnishi. Phys. Rev. Lett. **68**, 2898 (1992)

[23] A.K. Kermann and S.E.Koonin, Ann. Phys. **100** (1976) 332

[24] J. Singh, Ph. D. Thesis, Panjab University, Chandigarh, India (2001)

[25] Jatinder Kaur Dhawan, Ph. D. Thesis, Panjab University, Chandigarh, India (2007)

[26] G. Peilert *et al.,* Phys. Rev. C **39**, 1402 (1989); A. Bohnet, N. Ohtsuka, J. Aichelin, R. Linden and A. Faessler, Nucl. Phys. A **494**, 349 (1989); L. Neise *et al.*, Nucl. Phys. A **519**, 375c (1990); M. Berenguer *et al.*, J. Phys. G: **18**, 655 (1992); A. Bohnet *et al.*, Phys. Rev. C **44**, 2111 (1991)

[27] J. Singh, S. Kumar and R. K. Puri, Phys. Rev. C **62**, 044617 (2000); *ibid* **65**, 024602 (2002); R. K. Puri and S. Kumar, Phys. Rev. C **57**, 2744 (1998).

Chapter 3

Nuclear Stopping in Heavy Ion Collision

3.1 Introduction

A major goal of heavy-ion collisions (HIC) at intermediate energies is to extend our knowledge about the properties of hot and dense nuclear matter at extreme conditions. Nuclear reactions from low to relativistic energies provide variety of phenomena. As stated in Chap. 1, Pauli principle blocks majority of scattering of nucleons at low incident energies. Therefore, attractive mean field dominates the physics in this energy regime [1]. At intermediate energies, however, a mixture of attractive mean field and repulsive nucleon-nucleon scattering exists [2, 3]. Both these regimes together, lead the matter from a fused state to total disassembly. One is also interested to understand the mechanism behind this. Further, the origin of small pieces (fragments) is also of great interest. One is trying to correlate this origin with global stopping [4]. In the following, we shall discuss the phase-space simulations of heavy-ion collisions and then shall present our detailed analysis of global stopping reached in heavy-ion collisions by using an isospin dependent quantum molecular dynamics model (IQMD).

3.2 Time Evolution

In order to define more clearly the most relevant quantities for nuclear stopping in heavy-ion collisions, Figure 1 sketches schematically a typical heavy-ion reaction. When two nuclei approach each other, their orientation in space and their

initial beam direction define the reaction plane. The impact parameter vector b is located in the reaction plane.

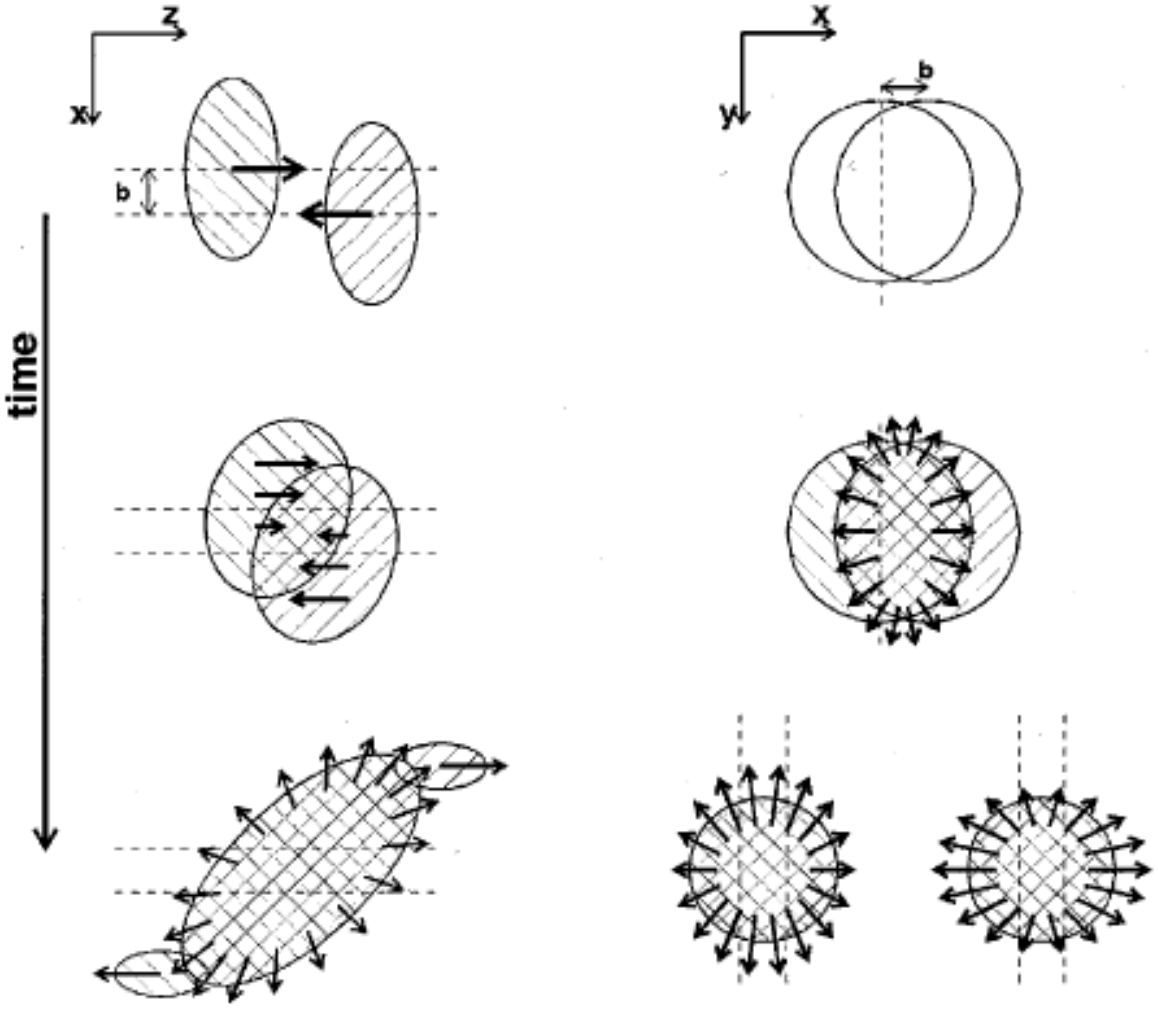

Figure 3.1: Schematic view of the time evolution in a heavy-ion collision. Left is the time evolution of the reaction in the reaction plane and right, a sketch of the transverse plane at midrapidity. Several phases of a typical heavy-ion reaction can be identified.

3.2.1 Initial Phase: When the two matter distributions approach each other and start to overlap, the properties of the nucleon-nucleon interaction in free space will be visible in the scattering process. Nucleons at the surfaces will reflect the Lorentz-force-like behavior of the nucleon-nucleon interaction most directly. They will be deflected outwards and because of symmetry for finite impact parameter, will show an enhancement in the reaction plane [5-7]

3.2.2 High-Density Phase: Once the matter distributions of the projectile and target overlap, the properties of the nucleon-nucleon interaction are not well known. For large systems and large enough cross-sections, the overlap zone develops into a system characterized by an initial baryon number and energy density [8, 9]. Depending on its EOS, which relates the pressure to the density and temperature, the overlap zone may reach conditions that are described by an average density and temperature. This process of heating and compressing is intimately questioned of stopping, namely how much energy of the original longitudinal motion is transferred into internal degree of freedom in the course of the reaction. Having stored part of the available energy in compression and thermal excitation, heavy-ion collisions produce unique conditions of nuclear matter that are accessible otherwise.

3.2.3 Expansion: the next stage in the reaction scenario is the relaxation of the energy density; the central system is undergoing expansion, thereby reducing the temperature and density. For symmetry reasons, the expansion is azimuthally symmetric for central collisions. For reactions with finite impact parameter, the system always expands into the direction of the largest gradients in density and temperature. Figure 3.1 reveals that, in transverse direction, the initial expansion is largest in the direction of the reaction plane. In longitudinal direction, the expansion scenario depends on the degree of stopping. For a high degree of stopping and given the fact that the nuclei are Lorentz contracted in this direction, the pressure gradient is largest along the beam direction; therefore the system relaxes predominantly longitudinally [10]. For a transparent system, the rapidity distributions are longitudinally broadened because of the initial distribution. In the limits of very high incident energy, this picture predicts a complete decoupling of longitudinal and transverse expansion [11]. For elastic collisions, this process is rescattering, and for inelastic collisions it leads to absorption. Provided the expansion is fast with respect to the longitudinal motion, nucleons participating in the expansion are absorbed preferentially in the reaction plane, where the spectator matter is present.

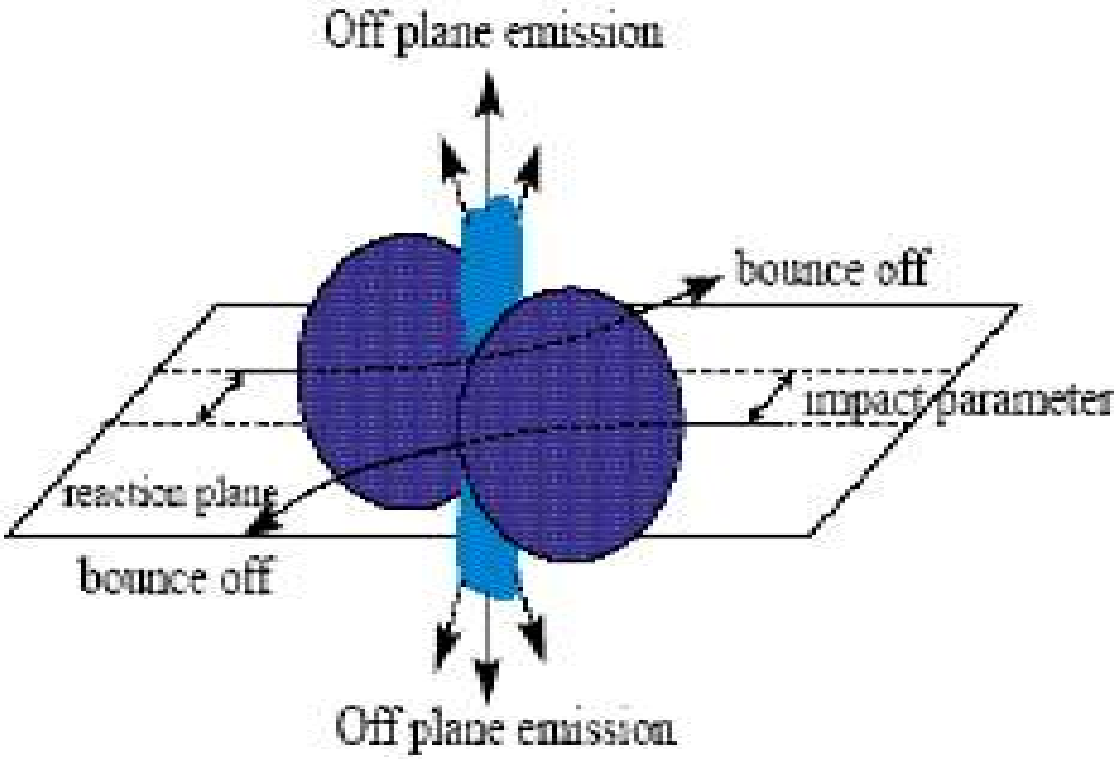

Figure 3.2: Display of the in-plane bounce off caused by compression and the squeeze out, the enhanced emission of light particles perpendicular to the reaction plane close to mid-rapidity.

3.2.4 Freeze-Out: The reaction and the development of collective signatures, stops at a point commonly referred to as freeze-out. At this point the densities are small enough that during a typical path length no further interaction will occur. The properties of the system at freeze-out are well known from the systematic study of particle ratios [12, 13].

On studying time-evolution in Heavy-ion collision and looking at figure 3.2, we note that the central collisions lead to a complete spherical distribution. This degree of stopping decreases with the increase in impact parameter. Further, the light charged particles (LCP) mostly originate from the mid-rapidity region. In other words, LCP's can

also act as a barometer for studying the stopping in heavy-ion collisions. The intermediate mass fragments are, however, pointed towards either target or projectile regions. Therefore, these are originated from the surface of the colliding nuclei. In other words, these can be viewed as remnant of the spectator matter. It has been discussed by many authors that the intermediate mass fragments carry the initial memory of nuclei and correlations. Naturally, one cannot expect them to be emitted from mid-rapidity region. Since degree of spectator matter increases with impact parameter, so is the formation of either IMF's or heavier fragments.

3.3 Global Stopping

The global stopping is defined as the randomization of one-body momentum space or memory loss of the incoming momentum. The degree of stopping, however, may vary drastically with incident energies, mass of colliding nuclei and colliding geometry. The degree of global stopping has also been linked with the thermalization (equilibrium) in heavy-ion collisions. A complete knowledge about the degree of stopping is very important since it can be connected to the properties of the system equation of state and in medium properties of the nucleon-nucleon cross-section [14].

Theoretically, these happenings are followed by a variety of models. Some models assume a *priori* equilibrium (at least at local level) whereas others hunt for the degree of thermalization in a reaction. Several models which depend on the assumption of equilibrium have been applied successfully to study the physics at low and intermediate energies [15, 16]. At the same time, the light and medium mass fragments (produced and emitted in reactions), have also been used to get information about the thermalization and stopping in heavy-ion collisions [4, 17]. The origin of light and medium mass fragments is still under debate.

The colliding nuclei not only compress each other, they also heat the matter [18]. In addition, the destruction of initial correlations makes the matter homogeneous

and one can have global stopping. More the initial memory of nucleons is erased, better it is stopped and better one has average mixing of projectile and target momentum. We shall here consider few different quantities capable of estimating the degree of global stopping.

After early studies of stopping in proton and light-ion–induced reactions (for reviews see (19, 20)), most studies have concentrated on symmetric collision systems. If complete overlap is reached in such collisions and stopping is large, then such systems are ideal for studying the free expansion of hot and dense nuclear matter into the vacuum. For rather small systems, if just two nucleons out of the target and projectile are not participating in a particular collision, about 4% of the available center-of-mass (c.m.) energy is already unavailable in that collision. In heavy symmetric systems (Au + Au or Pb + Pb), the region of overlap for the outer and less dense surface of the nuclei is large, and again it is difficult to pick out collisions where these regions have full overlap.

Nevertheless, there exist strategies for finding the most central collisions. One strategy is to require a combination of observables, for example, large charged-particle multiplicity and small directivity, i.e. a symmetric momentum distribution of the emitted particles [21]. Another possibility is to select high multiplicity in conjunction with a large ratio of transverse energy to longitudinal energy [22]

Nuclear stopping in heavy ion collision (HIC) has been studied by means of rapidity distribution [23] and asymmetry of nucleon momentum distribution [24-26]. It is an important quantity in determining the outcome of a reaction [27, 28]. Nuclear stopping can be used as a new probe to extract the information on the Isospin dependence of in-medium nucleon-nucleon cross section in intermediate energy heavy ion collisions.

3.4 Parameters for describing Nuclear Stopping in Heavy ion collision:

The following quantities can be used to describe nuclear stopping in Heavy Ion collision:

3.4.1 Quadrupole Moment

The momentum quadrupole Q_{ZZ} is defined as

$$Q_{ZZ} = \sum_i^A [\, 2P_Z(i)^2 - P_x(i)^2 - P_y(i)^2 \,] \qquad (3.2)$$

Here the total mass A is the sum of the projectile mass A_P and the target mass A_T. From the expression, it is clear that for spherical distribution of momentum, Quadruple moment Q_{zz} vanishes. For a complete stopping, Q_{zz} should be close to 0. It implies $1/Q_{zz}$ must have larger value for complete stopping. It has been observed that with the passage of time, when the beam energy is less, the asymptotic value of Q_{zz} decreases towards zero, indicating an isotropic nucleon momentum distribution of the whole composite system and consequently a full stopping at beam energy below Fermi energy. As beam energy increases above Fermi energy, because of the pre-equilibrium particle emission and target like nuclei, Q_{zz} will get certain non-vanishing value, indicating partial transparency. The relaxation time decreases as increasing beam energy, which shows the fact that high energy leads to more violent N-N collisions and faster dissipation. This is consistent with the Isospin equilibrium process as shown by Li *et al.[*29]

3.4.2 Anisotropy Ratio R (Stopping ratio)

Another possibility of degree of stopping is the anisotropy ratio which is the

transverse-parallel ratio of momentum (*R)* given by

$$R = \frac{2}{\pi}\left(\frac{\sum_i^A |P\perp(i)|}{\sum_i^A |P_{\text{II}}(i)|}\right) \tag{3.3}$$

The values of the transverse and parallel (longitudinal) components of the momentum of the i^{th} nucleon are

$$P_\perp(i) = \{ P_x(i)^2 + P_y(i)^2\}^{1/2} \tag{3.4}$$

and $$P_{||}(i) = P_\perp(i) \tag{3.5}$$

respectively. Naturally for a complete stopping, R ratio should be close to unity. More close is the value of R to one, more is the stopping in colliding nuclei. Super-stopping leads to $R > 1$ while large transparency leads to $R < 1$.

3.4.3 Rapidity Distribution

Stopping is a measure of the efficiency of converting the incoming longitudinal energy of a projectile and target into transverse degree of freedom, hence slowing down of incoming nucleons. The signatures of incomplete stopping and of a longitudinally expanding source lead to similar rapidity distributions of the emitted particles. One way to distinguish collective longitudinal expansion from incomplete stopping is to look at central collisions of projectiles and target with very different N/Z ratios. Incomplete stopping is indicated if distributions of neutrons and protons (including those bound in fragments) in the beam rapidity regime still resemble the Isospin composition of the incoming projectile. A symmetric central collision with a high degree of stopping can be viewed as a thermalized fireball sitting at rest in the c.m. frame, i.e. at midrapidity. The degree of stopping of nuclear matter can be studied from rapidity distribution which is defined as

$$Y(i) = \frac{1}{2}\ln\frac{E(i)+p_z(i)}{E(i)-p_z(i)} \tag{3.6}$$

Where $E(i)$ and $p_z(i)$ are, respectively, the total energy and longitudinal momentum of i^{th} particle. Naturally, for a complete stopping, one should expect a single Gaussian shape of the rapidity. More is the value of single shaped Gaussian at $Y_{c.m.}/Y_{beam}$ = 0, more is the nuclear stopping. Very often, the nature of emitting source is defined by analyzing the rapidity distribution. Apart from the global stopping and randomization of phase-space, one may also define the local average mixing of target and projectile.

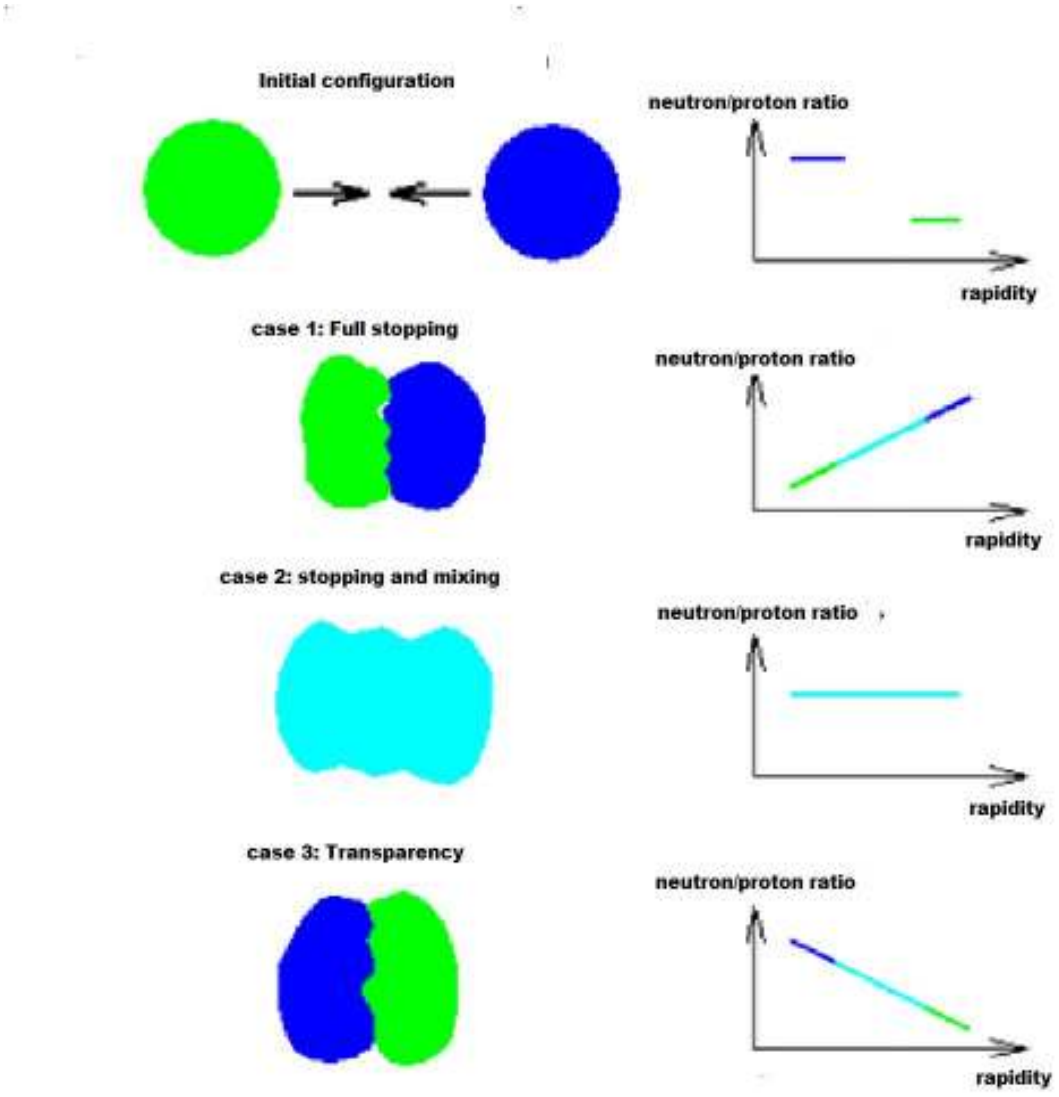

Figure 4.3: Illustration of using the rapidity distribution of neutron/proton ratio as a probe of nuclear stopping power.

If two nuclei collide three different scenarios are possible:

1. The nuclei are repelled off by each other like in the collision of two hard spheres.
2. The nuclei are compressed and mix up like in the collision of two (compressible) droplets.
3. The nuclei are passing each other without much interaction like two large crowds of bees.

The different scenarios would cause different longitudinal momentum distributions for the projectile and target particles. This may be studied by regarding isotopic ratios in the reaction of projectiles and target with different Z/A. The stopping of nuclear matter is necessary to create a hot compressed region at the centre of the reaction. This region may then repell the following incoming particles and thus causes nuclear flow

3.4.4 Transverse Momentum

Transverse momentum P_T is given by

$$P_T = \sqrt{(p_{1x} + p_{2x})^2 + (p_{1y} + p_{2y})^2} \quad (3.7)$$

The strength of transverse flow is examined as a function of transverse momentum P_T. P_T dependence reveals useful information about the collective flow that is complementary to that obtained from the standard in-plane transverse momentum analysis. Quadrupole moment Q_{zz} and Anisotropy ratio R, i.e. the ratio of transverse to longitudinal momentum values, as a function of transverse momentum are very sensitive to the medium modifications of the cross sections.

To study the Nuclear Stopping in Heavy Ion collision, we will analyse the dependence of transverse momentum P_T and rapidity distribution on quadrupole moment Q_{zz} and stopping ratio R (anisotropy ratio) by studying reactions of Cr and Ni with varying N/Z ratio in the energy range 50 MeV/nucleon to 200 MeV/nucleon.

References

[1] L. C. Vaz *et al.,* Phys. Rep. **69**, 373 (1981); R. K. Puri, Ph. D. Thesis, Panjab University, Chandigarh, India (1990).

[2] H. Stöcker and W. Greiner, Phys. Rep. **137**, 277 (1986).

[3] J. Aichelin, Phys. Rep. **202**, 233 (1991); C. Hartnack *et al.*, Eur. Phys. J. A **1**, 151 (1998).

[4] P. B. Gossiaux and J. Aichelin, Phys. Rev. C **56**, 2109 (1997).

[5] C. Gale, G. Bertsch, S. Dasgupta, Phys. Rev. C **35**, 1666 (1987)

[6] J. Aichelin, *et al.,* Phys. Rev. Lett. **58**, 1926 (1987)

[7] B. Blattel, *et al.,* Phys. Rev. C **43**, 2728 (1991)

[8] C. M. Ko, G. Q. Li, J. Phys. G **22**, 1673 (1996)

[9] W. Cassing, E. L. Bratkovskaya, Phys. Rep. **308**, 65 (1999)

[10] L. D. Landau, Izv. Akad. Nauk, Ser. Fiz. **17**, 51 (1953)

[11] J. D. Bjorken, Phys. Rev. D **27**, 140 (1983)

[12] P. Braun-Munzinger, J. Stachel, J. P. Wessels, N. Xu, Phys. Lett. B **344**, 43 (1995)

[13] P. Braun-Munzinger, J. Stachel, J. P. Wessels, N. Xu, Phys. Lett. B **365**, 1 (1996)

[14] P. Danielewicz, Acta Phys. Polon. B **33**, 45 (2002); B. Hong *et al.*, Phys. Rev. C **71**, 034902 (2005); T. Gaitanos, C. Fuchs and H. H. Wolter, Phys. Lett. B **609**, 241 (2005).

[15] J. P. Bondorf *et al.*, Nucl. Phys. A **443**, 321 (1985); D. H. E. Gross, Rep. Prog. Phys. **53**, 605 (1990).

[16] L. G. Moretto and G. J. Wozniak, Annu. Rev. Nucl. Part. Sci. **43**, 379 (1993).

[17] J. Lukasik *et al.*, Phys. Rev. C **55**, 1906 (1997); *ibid*, Phys. Rev. C **61**, 014606 (1997); *ibid*, Phys. Rev. C **66**, 064606 (2002); T. Lefort *et al.*, Nucl. Phys. A **602**, 397 (2000); F. Rami *et al.*, Phys. Rev. Lett. **84**, 1120 (2000); W. Reisdorf *et al.*, Phys. Rev. Lett. **92**, 232301 (2004).

[18] D. Hahn and H. Stöcker, Nucl. Phys. A **476**, 718 (1988); D. T. Khoa *et al.*, Nucl. Phys. A **542**, 671 (1992); R. K. Puri *et al.*, Nucl. Phys. A **575**, 733 (1994).

[19] W. Busza, R. Ledoux, *Annu. Rev. Nucl. Part. Sci.* **38**, 119 (1988)

[20] J. Stachel, G. R. Young, *Annu. Rev. Nucl. Part. Sci.* **42**, 537 (1992)

[21] J. P. Alard, *et al* (FOPI Collaboration). *Phys. Rev. Lett.* **69**, 889 (1992)

[22] S. C. Jeong, *et al* (FOPI Collaboration). *Phys. Rev. Lett.* **72**, 3468 (1994)

[23] C.Y. Wong, *Introduction to High-Energy Heavy-Ion Collisions* (World Scientific, Singapore, 1994).

[24] B. A. Li and C. M. Ko, Nucl. Phys. A **601**, 457 (1996).

[25] F. Videbaeck and O. Hansen, Phys. Rev. C **52**, 2684 (1995).

[26] W. Bauer, Phys. Rev. Lett**. 61**, 2534 (1988).

[27] W. Busza and R. J. Ledoux, Annu. Rev. Nucl. Part. Sci. **38**, 119 (1988).

[28] B. A. Li and C.Y. Wong, Phys. Scr. V **47**, 151 (1993).

[29] B. A. Li, C. M. Ko, and W. Bauer, Int. J. Mod. Phys. E **7**, 147–229 (1998).

Chapter 4

Results and Discussion

4.1 Introduction

Simulation has been carried out using IQMD model for 5000 events for $^{52}Cr_{24}$ + $^{54}Ni_{28}$, $^{52}Cr_{24}$ + $^{56}Ni_{28}$, $^{52}Cr_{24}$ + $^{58}Ni_{28}$, $^{52}Cr_{24}$ + $^{60}Ni_{28}$, $^{52}Cr_{24}$ + $^{62}Ni_{28}$ at different beam energies from 50 to 200 MeV/nucleon at non-central collisions. Soft equation of state (EOS) has been employed with symmetry energy E_{sym} = 32 MeV and compressibility κ =200 MeV. Nearly, symmetric reactions are chosen to avoid the influence of the asymmetry of colliding nuclei. We shall work out the effect of neutron rich target on degree of stopping and the emission of fragments. It will be of interest to see how large number of neutrons in the system affects the stopping. These particles are detected with minimum spanning tree (MST) method, in which binding in nucleons is possible if they are within a distance of 4 fm.

4.2 Dependence of Quadrupole Moment on Transverse momentum P_t

In fig 4.1, a non-central collision at impact parameter $\hat{b}$=0.1 and $\hat{b}$=0.3 has been displayed for the reaction $^{52}Cr_{24}$ + $^{54}Ni_{28}$ for different mass fragment. In the fig, top, middle and bottom are showing variation of Q_{zz} for free particles [A = 1], light mass fragments (LMF) [$2 \leq A \leq 4$] and intermediate mass fragments (IMF) [$5 \leq A \leq \frac{A_{tot}}{6}$] for different curves corresponds to energies ranging from 50 to 200 MeV/nucleon.

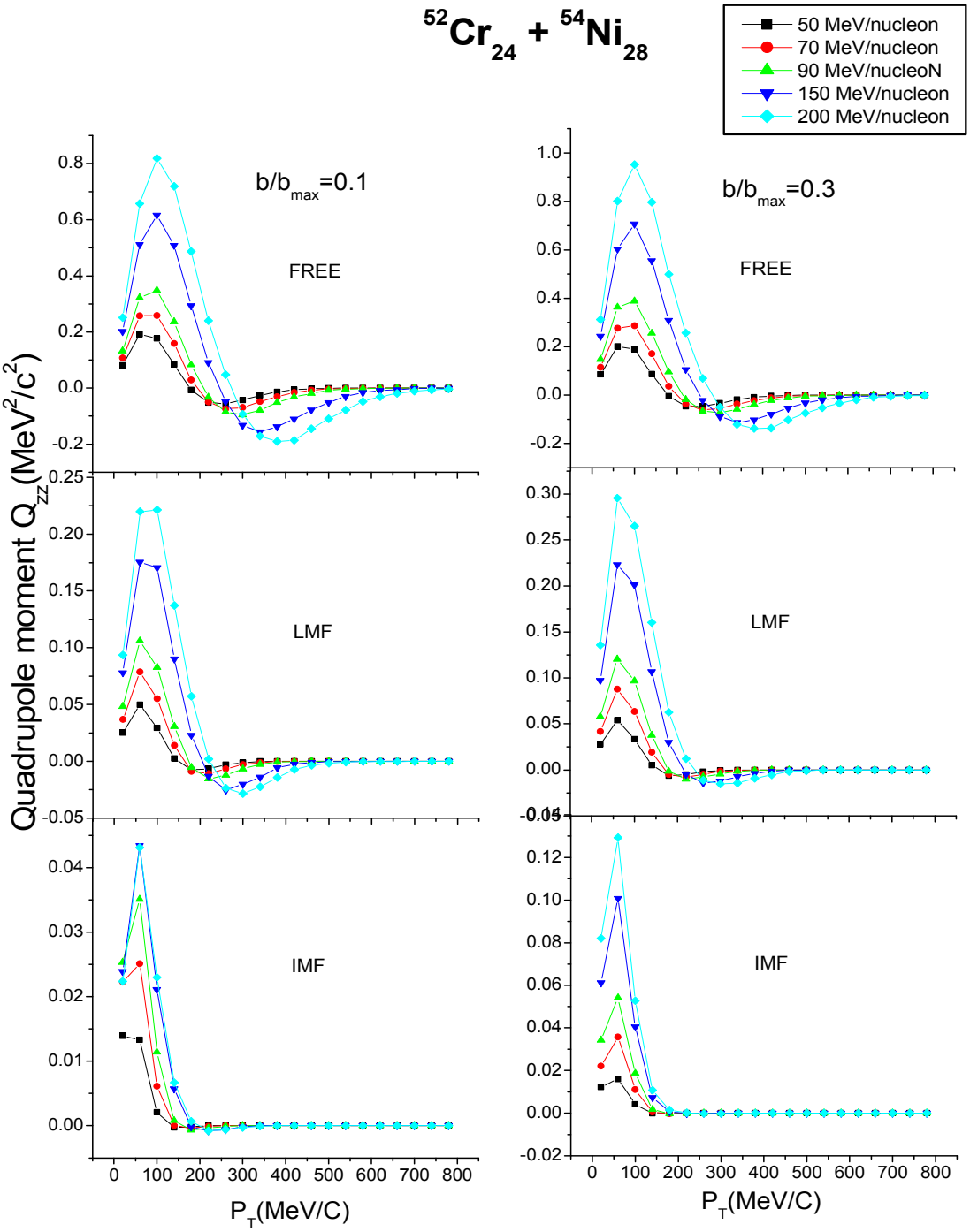
$^{52}Cr_{24}$ + $^{54}Ni_{28}$
50 MeV/nucleon
70 MeV/nucleon
90 MeV/nucleoN
150 MeV/nucleon
200 MeV/nucleon
b/b$_{max}$=0.1
b/b$_{max}$=0.3
FREE
LMF
IMF
Quadrupole moment Q$_{zz}$(MeV^2/c^2)
P$_T$(MeV/C)

Figure 4.1: Quadrupole moment as a function of transverse momentum P_T for the reaction $^{52}Cr_{24}$ + $^{54}Ni_{28}$ for $\hat{b}$=0.1 and $\hat{b}$=0.3.

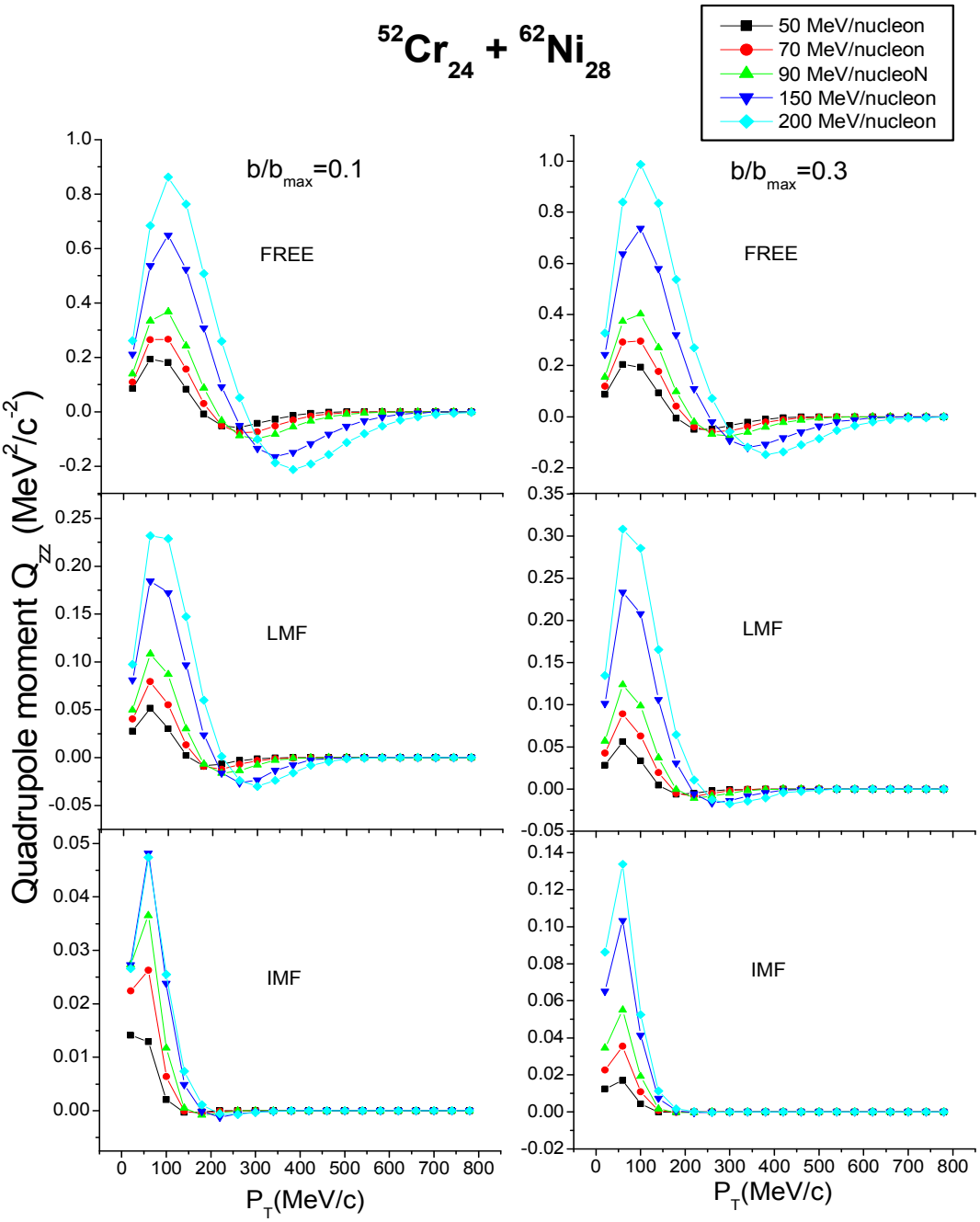

Figure 4.2: Quadrupole moment as a function of transverse momentum P_T for the reaction $^{52}Cr_{24}$ + $^{62}Ni_{28}$ for different energies at $\hat{b}$ = 0.1 and $\hat{b}$ = 0.3.

As we have said earlier, Q_{zz} should be equal to zero for complete stopping that means $1/Q_{zz}$ must have large value for larger stopping. Figure 4.1 shows the dependence of quadrupole moment Q_{zz} on transeverse momentum at $\hat{b}$=0.1 and $\hat{b}$=0.3. The value of Q_{zz} is maximum at largest energy for free, LMF's and IMF's. This is due to the fact that with increasing energy, the longitudinal component of momentum become stronger compared to transverse components. The value of Q_{zz} is compared for different values of impact parameter, i.e. $\hat{b}$=0.1 and $\hat{b}$=0.3. We observe that the value of Q_{zz} is more in the case of $\hat{b}$=0.3 and hence stopping will be less in this case.

Also the peak of Q_{zz} shifts to lower side as we go from free nucleon to intermediate mass fragments. This shows that heavy fragments have low transverse momentum associated with them.

Clear systematics can be seen that with increasing energy, the value of Q_{zz} increases. In the case of free particles, one can see the stopping decreases with increase in energy. Stopping is more effective at low energy.

Fig. 4.2 is same as fig. 4.1, but for $^{52}Cr_{24}$ + $^{62}Ni_{28,}$ the heaviest isotope of Ni has been taken into account to see the effect of increasing number of neutrons on quadrupole moment. One can see the difference produced in case of IMF's. On increasing the number of neutrons, the number of collisions will be suppressed and hence more is the quadrupole momentum associated with IMF's.

4.3 Quadrupole moment Q_{zz} as a function of energy

In figure 4.9, quadrupole moment Q_{zz} is plotted as a function of energy for the reaction $^{52}Cr_{24}$ + $^{58}Ni_{28}$ at impact parameter $\hat{b}$=0.1 and at t=200 fm/c. From the figure, it is observed that value of Q_{zz} for free nucleon and LMF increases with increase in energy. This means that stopping decreases with increase in energy. The production of free particles and LMF's increases with increase in energy and hence Q_{zz} show the

same behavior. This shows that stopping decreases with increase in energy. It has been reported in the literature that production of LMF's can be used as measure to predict the stopping in nuclear reaction.

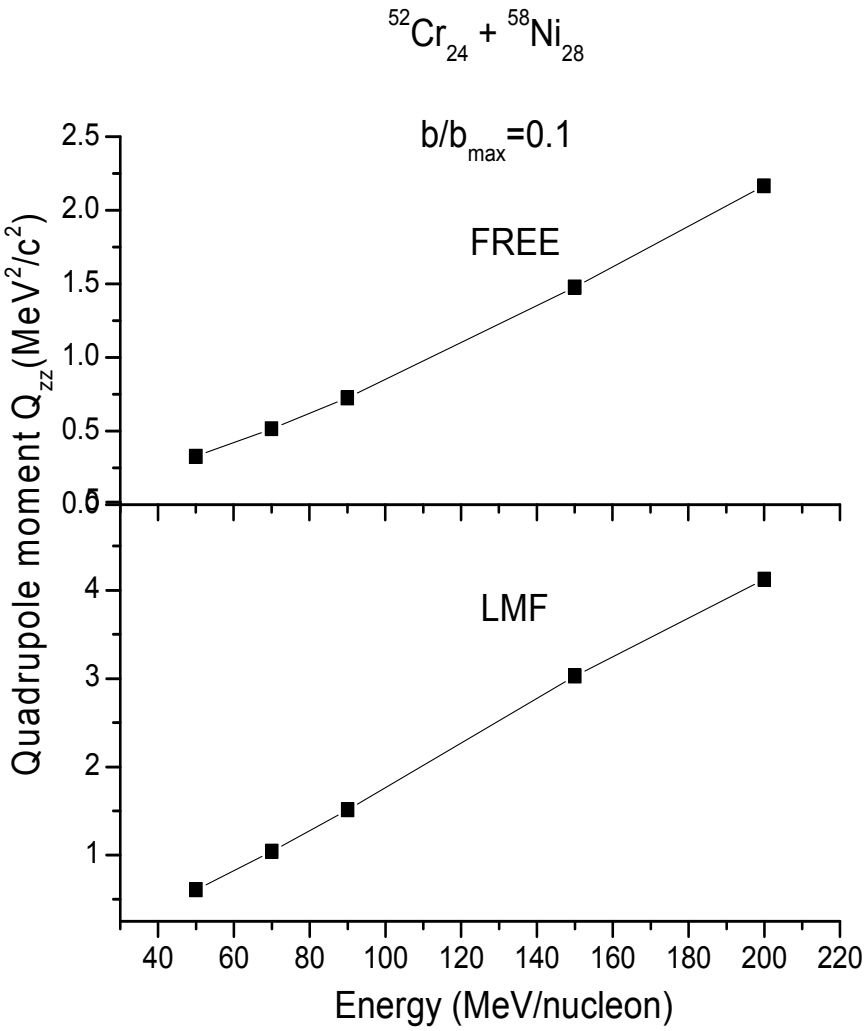

Figure 4.3: Quadrupole moment as a function of energy for the reaction $^{52}Cr_{24}$ + $^{58}Ni_{28}$ at impact parameter $\hat{b}$=0.1

4.4 Variation of Quadrupole moment Q_{zz} with N/Z

Figure 4.4 shows the variation of Q_{zz} with N/Z, i.e. neutron-proton ratio for free nucleons, LMF's and IMF's at t = 200 fm/c and $\hat{b}$=0.1 for different energies. The

effect of N/Z on stopping is weak. The value of Q_{zz} remains almost constant for a particular energy and its value increase with the increase in energy.

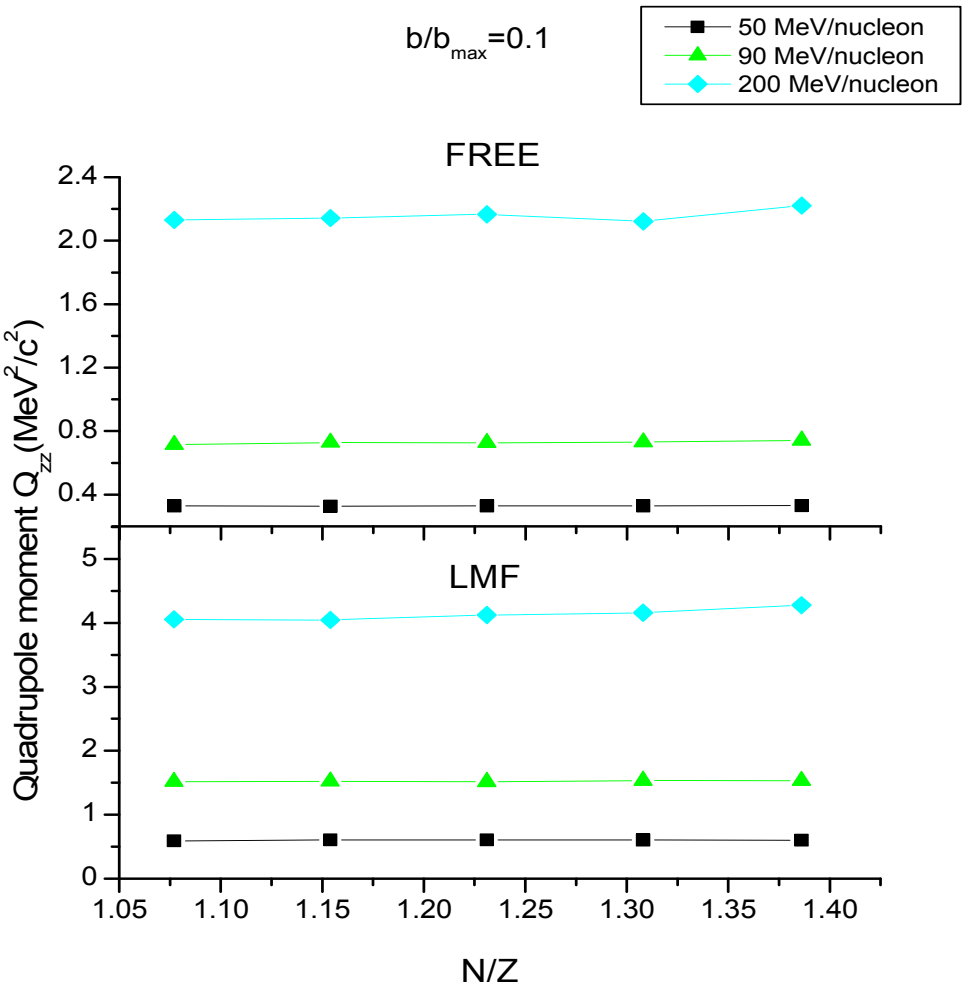

Figure 4.4: Quadrupole moment Q_{zz} as a function of N/Z at impact parameter $\hat{b}$ = 0.1

4.5 Variation of Quadrupole moment Q_{zz} with Impact parameter

Fig 4.5 shows the impact parameter dependence of Quadrupole moment Q_{zz} for neutron deficient and neutron rich systems at 50 MeV/nucleon and 200 MeV/nucleon

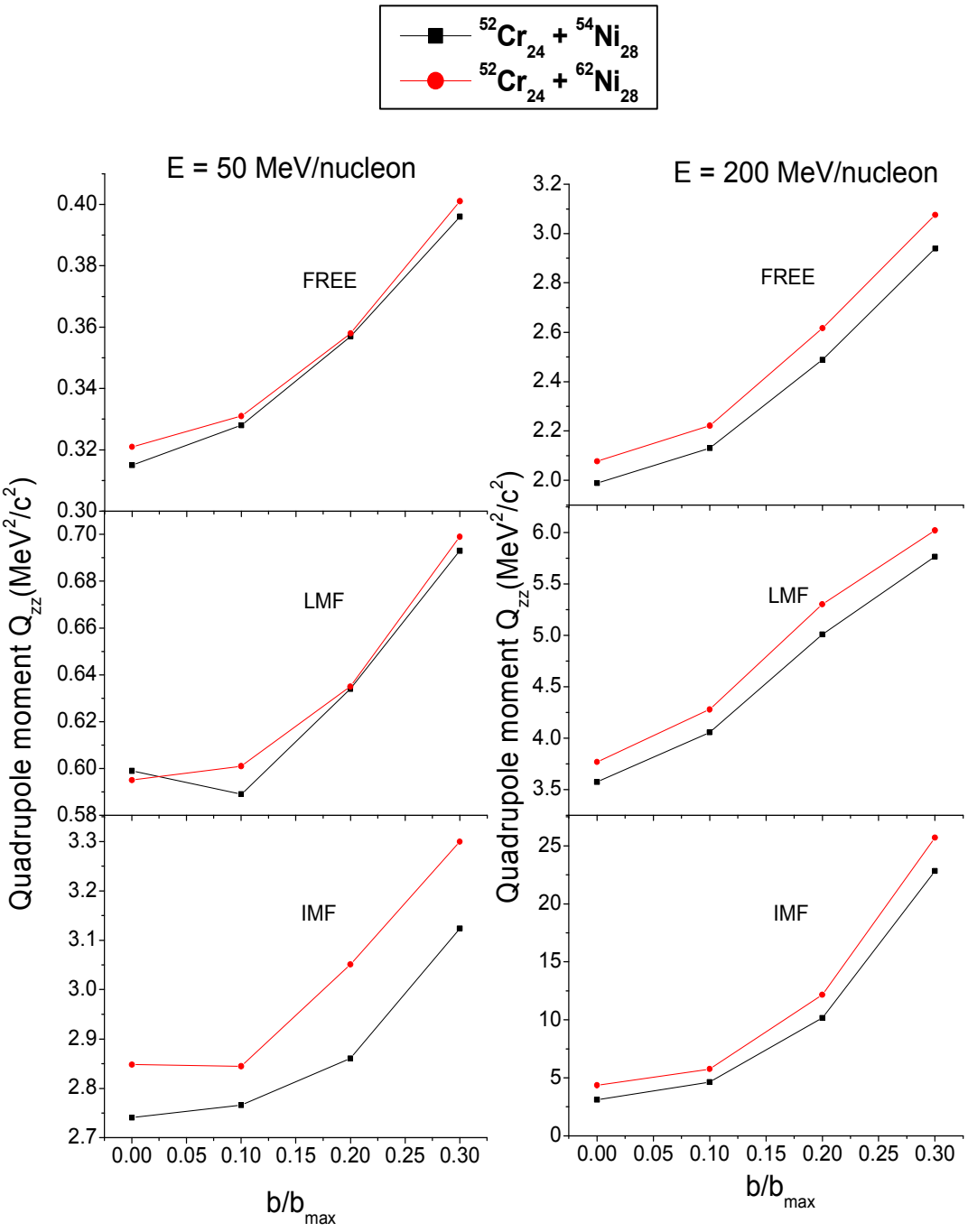

Figure 4.5: Variation of Quadrupole moment Q_{zz} with impact parameter for systems $^{52}Cr_{24}$ + $^{54}Ni_{28}$ and $^{52}Cr_{24}$ + $^{62}Ni_{28}$ at E = 50 MeV/n and 200 MeV/n.

The value of Quadrupole moment Q_{zz} increases with increase in impact parameter value. This is due to the fact that for lower value of impact parameter i.e. for $\hat{b}$=0, maximum number of collisions are possible and hence stopping is maximum. With the increase in the value of impact parameter, number of nucleons suffering collisions will decrease and hence stopping decreases.

4.6 Dependence of Stopping Ratio R on transverse momentum P_T

Figure 4.6 shows the variation of stopping ratio R with transverse momentum P_T at energies 50, 90 and 200 MeV/nucleon and for different impact parameters $\hat{b}$ = 0.1 and $\hat{b}$ = 0.3 for $^{52}Cr_{24}$ + $^{54}Ni_{28}$. The value of R is maximum for largest energy in case of free and LMF's. Large value of R contributes to the fact that transverse component of momentum is more than longitudinal component which leads to transverse flow of nucleons. Also, the peak of R shifts to lower side as we go from free nucleon to heavy mass fragments. This is because of low transverse momentum associated with heavy mass fragments.

On comparing for two different impact parameters, it is observed that stopping is more in case of $\hat{b}$ = 0.1. Because the smaller value of impact parameter will leads to larger the number of collisions and hence, maximum stopping will occur. Figure 4.7 shows the variation of R with transverse momentum for heaviest isotope of Ni i.e. for the reaction $^{52}Cr_{24}$ +$^{62}Ni_{28}$ to see the effect of increase in number of neutrons on stopping

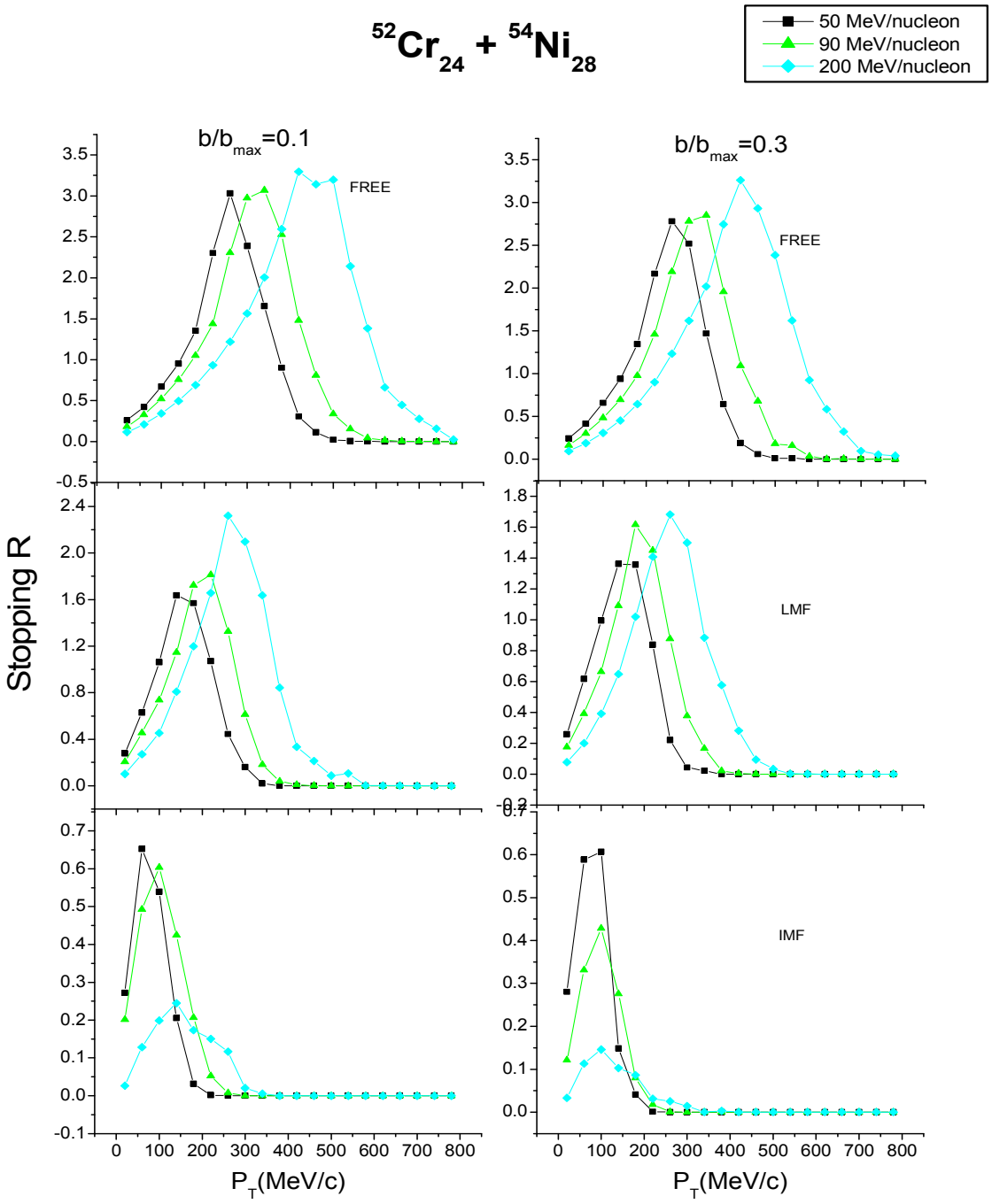

Figure 4.6: Stopping ratio R as a function of P_T (transverse momentum) for different energies for the reaction $^{52}Cr_{24}$ + $^{54}Ni_{28}$ for $\hat{b}$=0.1 and $\hat{b}$=0.3

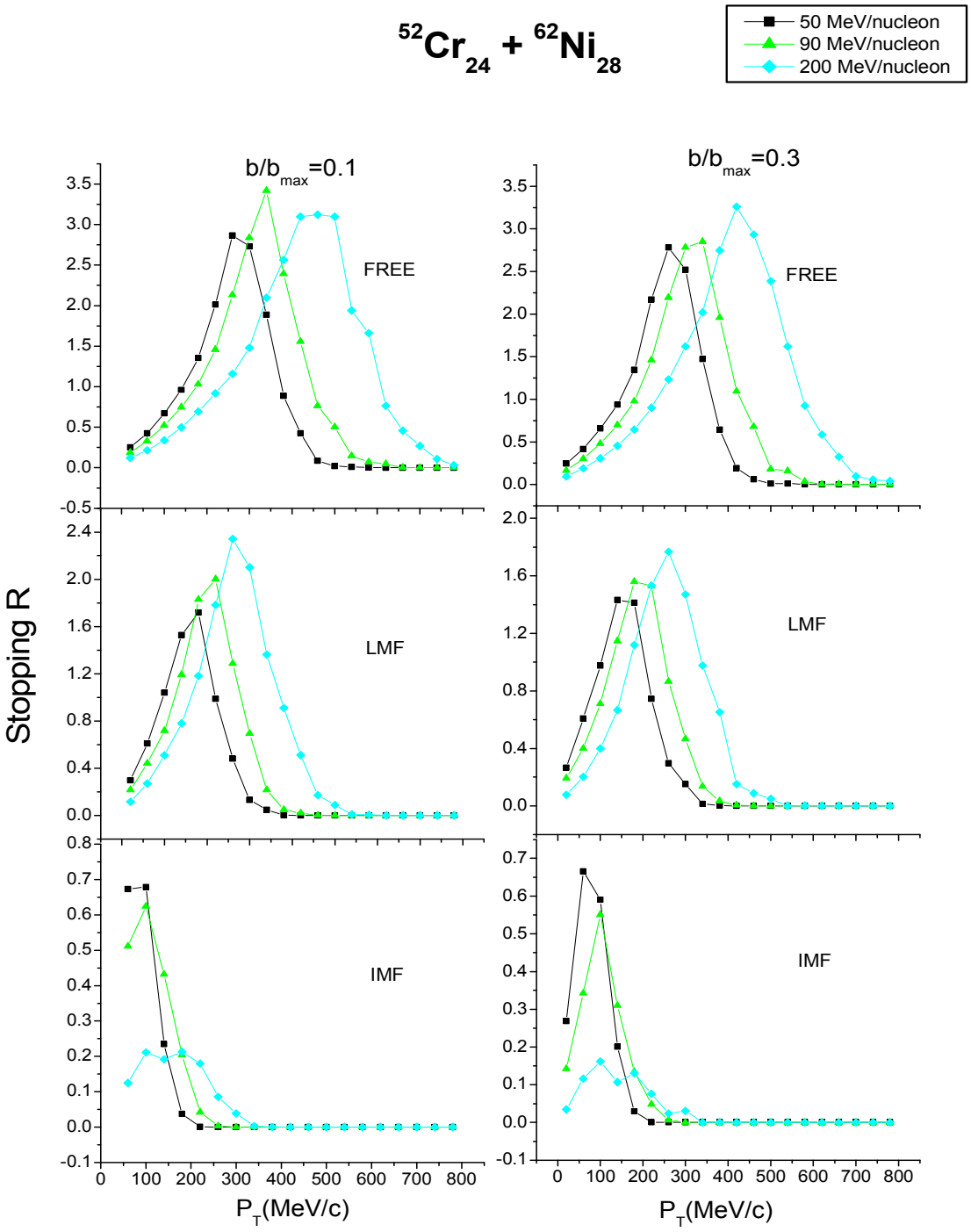

Figure 4.7: Stopping R as a function of transverse momentum for the reaction $^{52}Cr_{24}$ + $^{62}Ni_{28}$ at $\hat{b}$=0.1 and $\hat{b}$=0.3

4.7 Stopping ratio R as a function of rapidity

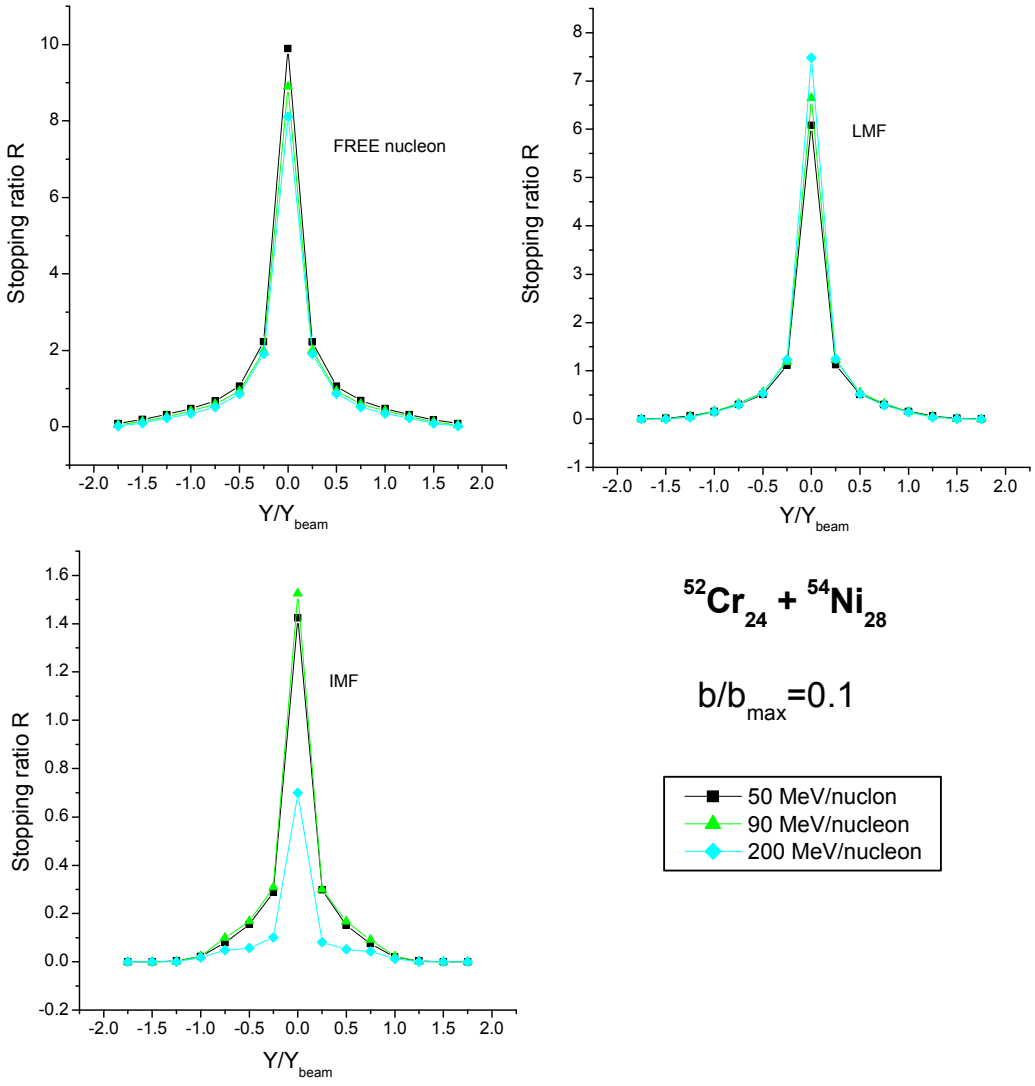

Figure 4.8: Stopping R as a function of rapidity for the reaction $^{52}Cr_{24}$ + $^{54}Ni_{28}$ at $\hat{b}$=0.1.

Figure 4.8 shows the stopping R as a function of rapidity for the reaction $^{52}Cr_{24}$ + $^{54}Ni_{28}$ at $\hat{b}$ = 0.1. There is a sharp peak obtained at mid-rapidity showing that value of stopping R is larger at mid-rapidity and decreases sharply on either side of mid-rapidity. In the mid-rapidity region, number of collisions is large, i.e. maximum stopping

is observed. The value of R decreases with increase in energy. This is due to the fact that with increasing energy, the transverse momentum associated with particles/fragments reduces and longitudinal component increases. Also the production of IMF's decreases with increase in energy and hence the value of R associated with IMF's decreases with increasing energy.

4.8 Stopping R as a function of incident energy

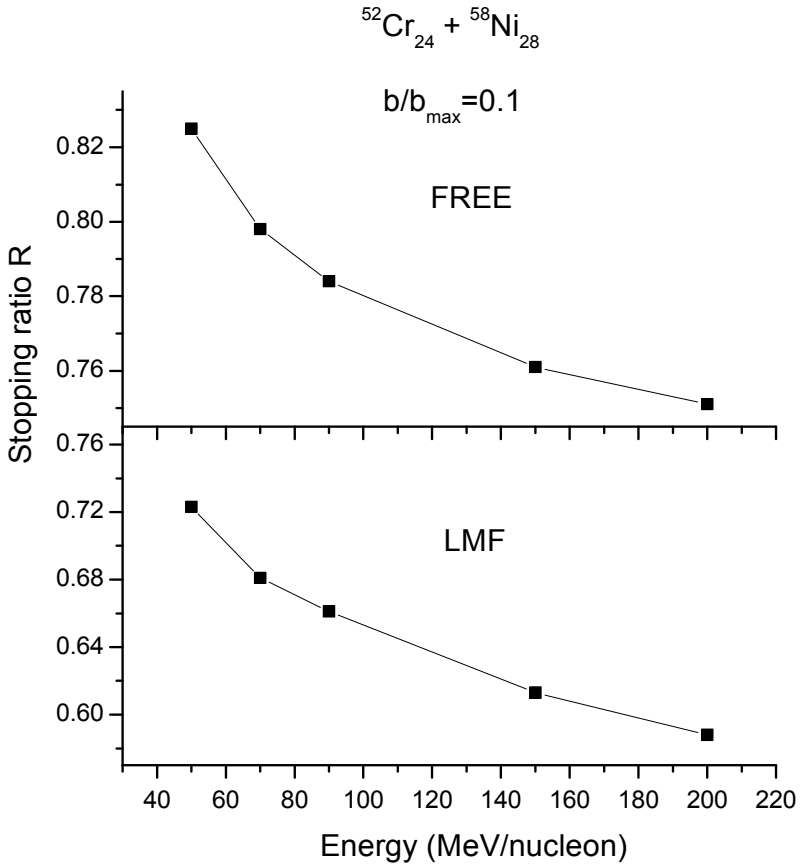

Figure 4.9: Stopping R as a function of incident energy for the reaction $^{52}Cr_{24}$ + $^{58}Ni_{28}$ at impact parameter $\hat{b}$=0.1

Figure 4.9 shows the variation of stopping ratio R with energy for free nucleons and LMF's. These are similar to the results reported in the literature. The value of R decreases with increase in energy for free nucleon and LMF's. The

transverse component associated with nucleon decreases as the energy increases. The stopping is more effective at low energy, but decreases with increase in energy.

4.9 Variation of stopping ratio R with N/Z

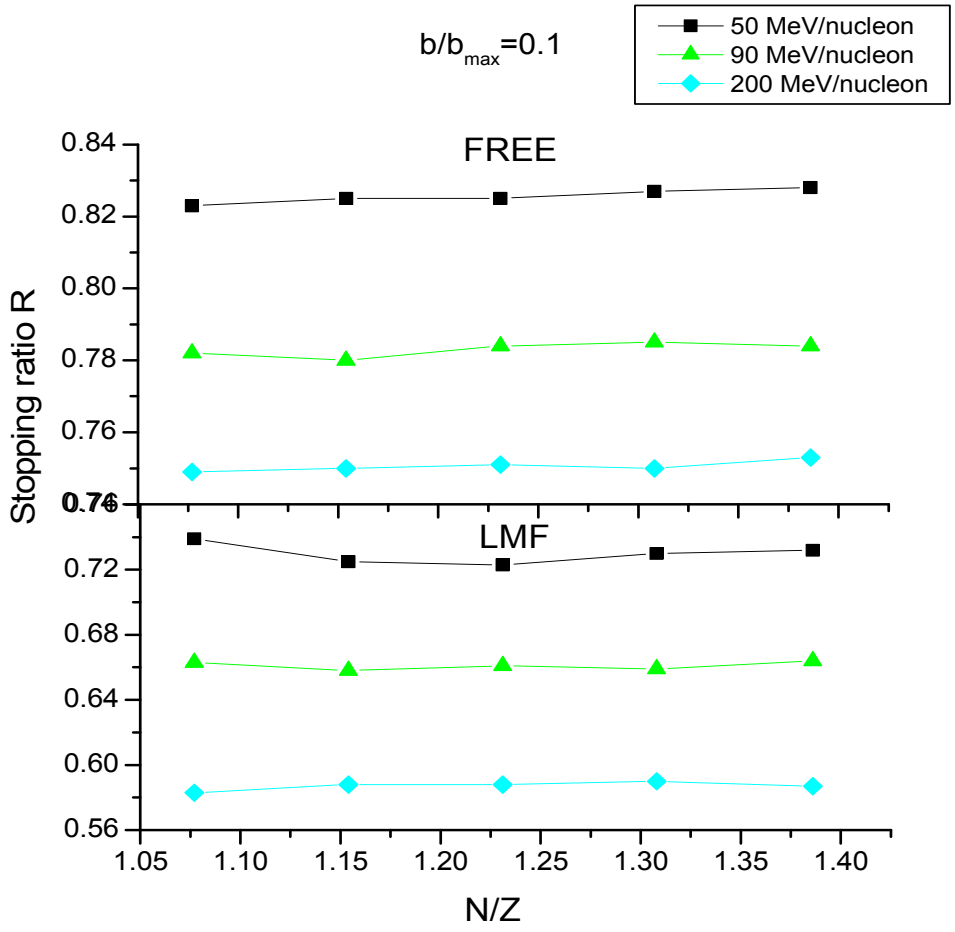

Figure 4.10: Stopping R as a function of N/Z for free and LMF for different energies at impact parameter $\hat{b}$=0.1

Figure 4.10 is a plot of stopping R as a function of N/Z at impact parameter $\hat{b}$ = 0.1. From the figure, it is observed that stopping ratio R behaves almost linearly with varying N/Z. The value of R decreases with increase in energy which is already shown in figure 4.9. So we can say that effect of N/Z on degree of stopping is weak.

4.10 Variation of stopping ratio R with Impact Parameter

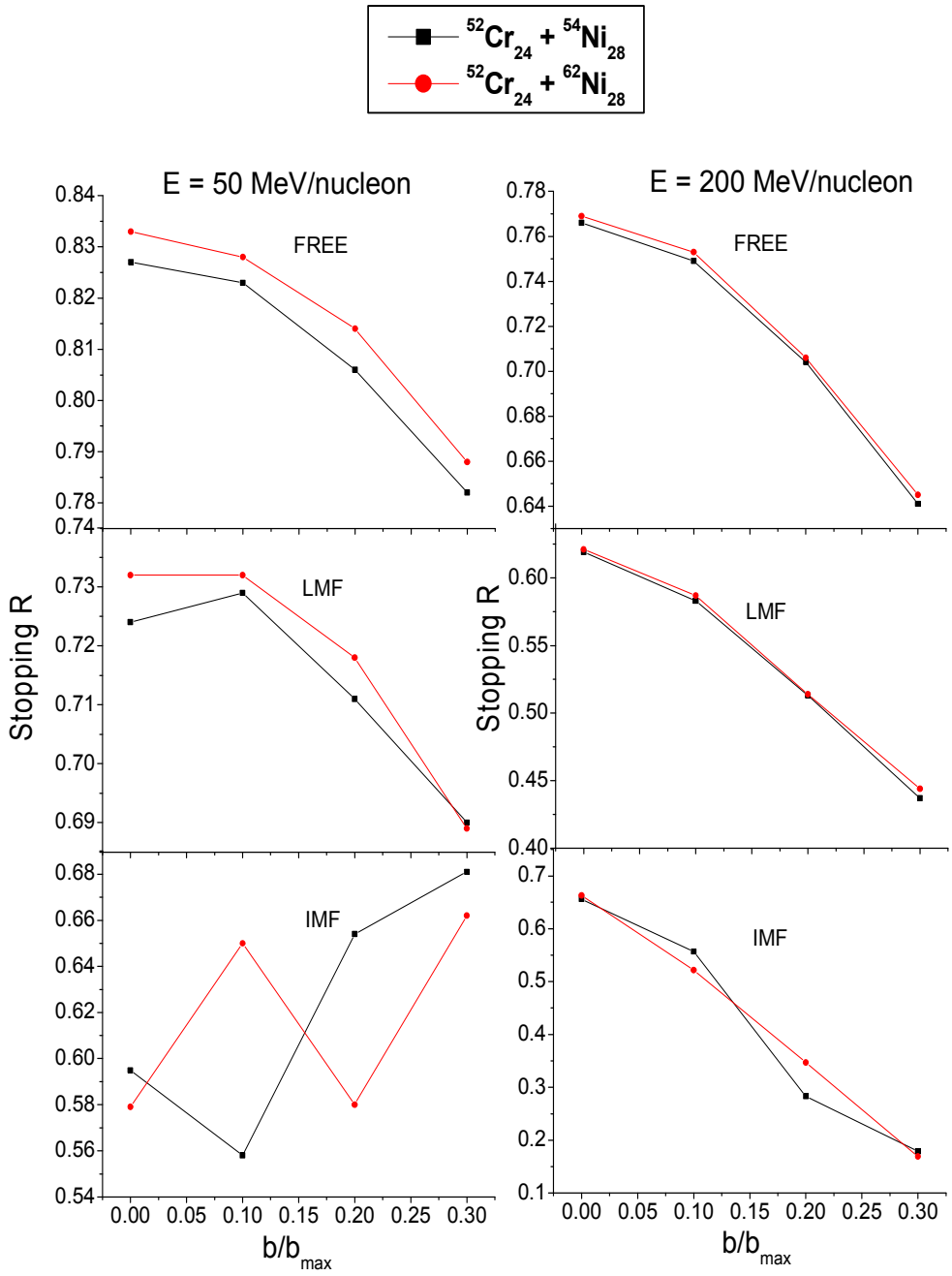

Figure 4.11: Variation of stopping ratio R with impact parameter for systems $^{52}Cr_{24}$ + $^{54}Ni_{28}$ and $^{52}Cr_{24}$ + $^{62}Ni_{28}$ at E = 50 MeV/nucleon and 200 MeV/nucleon.

Figure 4.11 shows the variation of stopping ratio R with impact parameter for systems $^{52}Cr_{24}$ + $^{54}Ni_{28}$ and $^{52}Cr_{24}$ + $^{62}Ni_{28}$ at E = 50 MeV/nucleon and 200 MeV/nucleon.

The value of R decreases with increase in impact parameter. Maximum value of R at b=0 implies maximum stopping in central collisions. For non-central collisions, stopping reduce. This is because in central collision, maximum number of nucleons can participate to undergo collisions. With increase in value of impact parameter, the probability for nucleons to undergo collisions will decrease.

4.10 Conclusions:

In chapter 4, we get following conclusions:

- Stopping is large in case of free particle emission. This is because of the reason that free particles emitted have high transverse momentum associated with them than LMF and IMF.
- Stopping R shows a sharp peak maximum in mid-rapidity region, while Quadrupole moment approaches approximately to zero which are basic conditions for large stopping to occur. Large number of collisions is observed in the mid-rapidity region. This is the region where most of particles act as participators. The region on either side of mid-rapidity belongs to the spectator particles.
- Quadrupole moment Q_{zz} and stopping R are varied with the incident energy. From the figures, it is clear that the stopping reduced with the increase in value of incident energy.
- Quadrupole moment Q_{zz} and stopping R shows a constant behavior with variation of N/Z. There is approximately no change in the value of Quadrupole moment and stopping with the increase in N/Z. So the effect of N/Z on degree of stopping is weak.
- With increase in impact parameter values, Quadrupole moment Q_{zz} increases while stopping ratio R decreases. This explains that stopping reduces with the increase in impact parameter.

Chapter 5

Summary

The thesis contains a theoretical study of nuclear stopping in heavy ion collision which is related with the phenomena like nuclear flow for hot and dense nuclear matter in heavy-ion collision at intermediate energies. The Isospin Dependent Quantum Molecular Dynamics (IQMD) model is used to describe the Isospin effect on nuclear stopping in intermediate energies.

In chapter 2, a brief review of various models like BUU, IBUU, Quantum Molecular Dynamics (QMD) model are presented. The Isospin Dependent Quantum Molecular Dynamics (IQMD) model is explained in details. Then method used for clusterization, i.e. Minimum Spanning Tree (MST) is discussed.

In chapter 3, there is complete theory of nuclear stopping in heavy ion collision. The parameters used to describe nuclear stopping like Quadrupole moment and Stopping or Anisotropy Ratio R are discussed along with a brief review on the dependence of these parameters on rapidity and transverse momentum.

Chapter 4 gives the analysis of the results obtained for describing nuclear stopping in heavy ion collision. Dependence of Quadrupole moment Q_{zz} and stopping R on transverse momentum, mid-rapidity, N/Z and energy are shown in figures for different mass fragments like free, light mass fragments (LMF) and heavy mass fragments (IMF).

In chapter 4, we get following conclusions:

- Stopping is large in case of free particle emission. This is because of the reason that free particles emitted are more momentum dependent than LMF and IMF. Heavy mass fragments are least momentum dependent. So stopping reduced in heavy mass fragments.

- Stopping R shows a sharp peak maximum in mid-rapidity region, while Quadrupole moment approaches approximately to zero which are basic conditions for large stopping to occur. Large number of collisions is observed in the mid-rapidity region. This is the region where most of particles act as participators. The region on either side of mid-rapidity belongs to the spectator particles.
- Quadrupole moment Q_{zz} and stopping R are varied with the incident energy. This variation explains that the stopping reduced with the increase in value of incident energy.
- Quadrupole moment Q_{zz} and stopping R shows a constant behavior with variation of N/Z. There is approximately no change in the value of Quadrupole moment and stopping with the increase in N/Z. So the effect of N/Z on degree of stopping is weak.
- With increase in impact parameter values, Quadrupole moment Q_{zz} increases while stopping ratio R decreases. This explains that stopping reduces with the increase in impact parameter.

Summarizing, an attempt has been made to describe nuclear stopping in heavy-ion collision, its dependence on different parameters and to study the nuclear flow, momentum correlations and degree of stopping.